Non-standard light for ultrafast laser microand nano-structuring

François Courvoisier

Non-standard light for ultrafast laser micro- and nano- structuring

Francois Courvoisier

This is a pre-peer-review version of a book chapter published in Stoian, R. and Bonse, J. (eds) "Ultrafast Laser Nanostructuring. The pursuit of extreme scales". Springer Series in Optical Sciences, vol 239. Springer, Cham.
The final version is available online at:
https://doi.org/10.1007/978-3-031-14752-4_16

Abstract Ultrashort laser pulses have revolutionized laser-matter interaction because they can deposit energy at extremely small scales. High speed and controlled nano structuring has become possible both at the surface of materials and inside transparent materials. We review here a specific class of beams, the "Bessel beams" that are quasi-invariant along the propagation. They provide new avenues for controlling laser matter interaction at extreme nanometric scales at the surface of materials but also within the bulk of transparent dielectrics. Of particular interest is the possibility to generate extremely high aspect ratio nano-structures, up to several 10 000:1 using single ultrafast laser pulses. The generation of nanoplasma using quasi-non-diffracting beams, provides access to extreme material states and opens a drastically new regime for material nano-structuring. In this chapter, we review the state-of-the-art of the fundamental concepts of Bessel beams and their applications, particularly for high aspect ratio nano structuring, drilling and stealth dicing. More complex beam shapes, based on the same concept of conical flow of light, offer new perspectives for materials processing.

Introduction

Chirped pulse amplification has enabled a evolution in laser structuring. High energy, ultrafast laser pulses, *i.e.* , with pulse duration typically between 50 fs to some tens of picoseconds, can generate a highly excited free-electron gas in the cold lattice. This is possible not only in metals but also in dielectrics, thanks to the nonlinear ionization. At the surface of materials, the ultrafast character of the energy deposition produces a high contrast between the excited zone and the non-excited material. This opens the possibility to structure materials at the micro- or nano- meter scale. This chapter will particularly emphasize the structuring of transparent materials bulk at

this extreme scale. One of the key aspects of the possibility to excite transparent materials via nonlinear ionization, is that energy can be stored inside the bulk of the material with no modification on the other surfaces. Femtosecond and picosecond lasers have therefore found a large number of applications during the last decade.

While early works were dedicated to inscribing in materials the tiniest modifications using highly focused Gaussian beams, it has been then recognized that beam shaping could bring new opportunities. Chapters 14 and 23 discuss the applications of beam shaping for laser micro-nano structuring. Here, we focus on a specific class of beam shapes which is the "non-diffracting" or "diffraction-free" beams. The terminology has been brought by Durnin when introducing the zeroth-order Bessel beam which is a propagation-invariant solution the wave equation [1]. The specificity of this beam is that it can maintain an extremely narrow focus, even below the wavelength, on extremely long distances, well beyond the limitation of the Rayleigh range. We will see that, in solid dielectrics, the zeroth-order Bessel beam has close links with the filamentation of ultrafast pulses.

A first class of applications therefore lies in the use of this propagation invariance to circumvent the technical issue of maintaining the workpiece surface within the laser focus. A second very important property of Bessel beams is that their nonlinear propagation inside transparent materials can be also invariant, in contrast with the nonlinear propagation of Gaussian beams which is conventionally much more difficult to control. We will see that the second property allows for depositing energy highly homogeneously along extremely long distances. The generation of extremely high aspect ratio nanostructures can be performed even using a single laser pulse. This has opened a large number of new applications. Among them, high-speed (meter per second) glass separation with a non-ablative process has attracted an enormous attention for obvious applications to mass fabrication of touchscreens, consumer electronics and more recently, for the high-speed cutting of windshields and window glass. This field of research has rapidly evolved from the first reviews [2, 3, 4, 5, 6].

In this chapter, we first describe in section 1 what are nondiffracting Bessel beams, how they can be shaped, and the applications of their extended focal zone to laser surface micro-nano-structuring. In section 2, we discuss the propagation of intense ultrashort pulses inside the bulk of transparent dielectrics. The nonlinear propagation of Bessel beams corresponds to the asymptotic behavior of the filamentation process of a Gaussian pulse. We show that Bessel-shaped pulses can generate plasma rods with nanometric diameter over a length of several tens of micrometers to centimeters. The relaxation of a nano-plasma rod inside the transparent material, can generate an index modification, nano-gratings, or a void. We discuss there the physics of the interaction and of the void formation. In section 3, we review the applications to high aspect ratio micro-nano-structuring of transparent dielectrics, with a particular emphasis on stealth dicing. Section 4 is dedicated to the new perspectives in the field: further beam engineering maintains the diffraction free character without the cylindrical symmetry of the initial Bessel beam. Tailoring the beam structure can improve the stress field, with important applications to stealth dicing. Another important perspective is to engineer the ultrafast laser beam such that it can produce

curved profiles inside the transparent material: this can be used to avoid mechanical chamfering that is conventionally used to avoid chipping of glass.

1 Propagation of non-diffracting beams in vacuum. Application to surface laser nanopatterning

In this section, we first describe what are non-diffracting Bessel beams and the means to generate them. We then review the applications of their extended focus to surface nano-structuring.

1.1 Non-diffracting beams and spatial beam shaping of ultrashort pulses

Basics of Bessel beams.

A Bessel beam can be seen as a cylindrically-symmetric interference field : it is the coherent superposition of an infinite set of plane waves whose wavevectors are distributed on the generatrix of a cone. Durnin has formalized the Bessel beam as a solution to the Helmholtz equation: this solution is featured by an intensity distribution that is invariant along the propagation direction [1].

The monochromatic field scalar amplitude of the zeroth-order Bessel beam reads in cylindrical coordinates as:

$$A(r,z,t) = A_0 J_0(\frac{2\pi}{\lambda}\sin\theta r) e^{i\frac{2\pi}{\lambda}\cos\theta z} \tag{1}$$

where λ is the wavelength, A_0 a constant and θ is defined as the cone angle. This is the angle made by the wavevector with respect to the optical axis: the wavevector has a radial component $k_r^0 = \frac{2\pi}{\lambda}\sin\theta$ and a longitudinal component $k_z^0 = \frac{2\pi}{\lambda}\cos\theta$. It is apparent from the above equation that the intensity $|A|^2$ of the field is invariant with z.

Obviously, this solution carriers infinite energy. In practice, the transverse profile is apodized, and the length of the Bessel beam is therefore limited. To simplify the terminology, we will not make a difference between the ideal Bessel beams and the experimentally realized ones. In addition, unless explicitly specified, we will call "Bessel beam" the zeroth-order Bessel beam.

Figure 1 shows how the interference field defines the length over which the Bessel beam exists. It is also apparent that the number of lobes around the central core is, during the propagation, progressively increasing and then decreasing. The Bessel zone length is typically defined by : $Z_{\max} \sim w/\tan\theta$, where w is typically the waist of the input Gaussian beam.

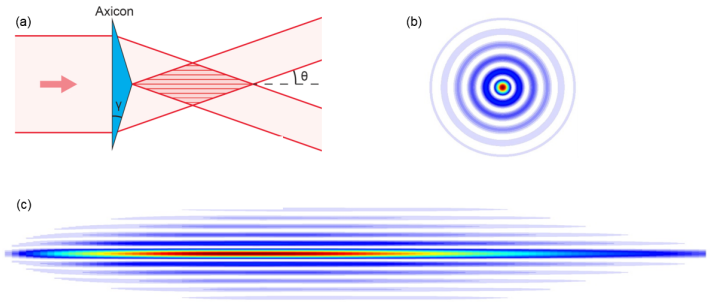

Fig. 1 (a) A Bessel beam is a cylindrically-symmetric field of interference and can be for instance generated using an axicon lens. (b) Example of a transverse cross section of the intensity distribution. (c) Longitudinal cross section of the intensity distribution.

Within the Bessel range, since the angle made by the interfering waves does not change along propagation, the central lobe diameter is invariant. The full width at half maximum of the central lobe intensity profile is $0.36\lambda/\sin\theta$, and the first zero of the intensity is given by: $r_0 = 0.38\lambda/\sin\theta$. In the Fourier space, *i.e.*, the far-field, the Bessel beam intensity distribution is a ring, peaked at $k_r = k_r^0$, with a thickness inversely proportional to the length of the Bessel zone.

A Bessel-Gauss beam is one of the experimentally realizable Bessel beams. It can be generated by shaping a Gaussian beam using an axicon. The on-axis intensity distribution of a Bessel-Gauss beam propagating in a medium of index n with a cone angle θ in the medium, can be expressed using the input power P_0 and waist w_0 of the Gaussian beam using the following expression, within the paraxial approximation [7, 8]:

$$I_{\text{on-axis}}(z) = 8\pi P_0 n z \frac{\sin^2\theta}{\lambda w_0^2} e^{-2(z\sin\theta/w_0)^2} \tag{2}$$

In the close vicinity of the central lobe, one can therefore approximate the Bessel-Gauss beam intensity profile to $I(r,z) = I_{\text{on-axis}}(z)|J_0(k_r^0 r)|^2$.

While for a Gaussian beam, the Rayleigh range shortens when the beam is more focused, *i.e.*, when the waist is smaller, the situation is very different for a Bessel beam since the cone angle θ and the waist w are two independent parameters. Therefore, the central core width can be down to nearly $\lambda/2$, while the Bessel zone length can be arbitrarily chosen – obviously within the limits of the numerical aperture of the optics –.

The Bessel beam can also be seen as an elongated focus, as it was initially shown by McLeod [9]. The energy flow is conical, and, within a geometric optics point of view, the energy is focused onto a segment instead of a point for the Gaussian beam. Increasing the length of the Bessel beam by a factor 10 only requires to increase the waist in a similar factor and, if one wants to maintain the peak intensity, the input power must be adequately increased.

Spatio-temporal structure

The spatio-temporal structure of the Bessel beam created using an ultrafast pulse is a coherent superposition of monochromatic Bessel beam amplitudes. The relationship between the different components is determined by the way the pulse is shaped. For instance, axicons or spatial light modulators do not create the same spatio-temporal structure [10]. However, to the best of our knowledge, the exact spatio-temporal structure of the Bessel beam has no impact on laser nano-structuring. This is why, in the following, we will treat the pulses using monochromatic approximation.

Presence of interfaces.

Importantly, when the beam crosses a flat interface at normal incidence such as air-dielectric or dielectric-air, the transverse profile does not change. This is because the radial wavevector is preserved [11]. The Bessel zone length is increased by a factor n, the refractive index of the medium. It is also important to highlight that the fact that the far field of the Bessel beam is composed only of a thin radial spectrum implies that the Bessel beam is much less sensitive to spherical aberration when the beam is focused inside a dielectric medium. This is an important benefit in comparison with Gaussian beams which are distorted in this situation.

Bessel beam generation

Bessel beams can be generated using several means. All are intended to apply a conical phase onto the Gaussian laser beam: spatial light modulators (SLM) [12, 13], diffractive optical elements [14, 15], transmissive [16, 17, 18, 19] or reflective axicons [20]. However, it is conventionally difficult to obtain high cone angle after such shaping means. Spatial light modulators and diffractive optical elements are limited to cone angles below some mrad. The fabrication of axicons is also technically very difficult, particularly when the cone angle is above some degrees. The mechanical turning often induces defects in the symmetry around the optical axis [21]. In addition, the tip of the axicon is very often rounded, which generates a spherical wave co-propagating and interfering with the Bessel beam [22, 23]. Recently-developed laser-based techniques avoid the defect of cylindrical asymmetry due to the mechanical interaction between the tool and the workpiece [24, 25].

As we will see below in section 2.4, the applications to nano-structuring often require strong focusing typically above 10 to 20°. Most of the high angle Bessel beam generators are similar to the one shown in Fig. 2. They are based on imaging a first Bessel beam using a 2f-2f telescopic arrangement which magnifies the cone angle at the cost of reducing the beam length by the square of the magnification. With this kind of architecture, the Bessel zone length is typically below a few hundreds of micrometers for a cone angle exceeding 10°.

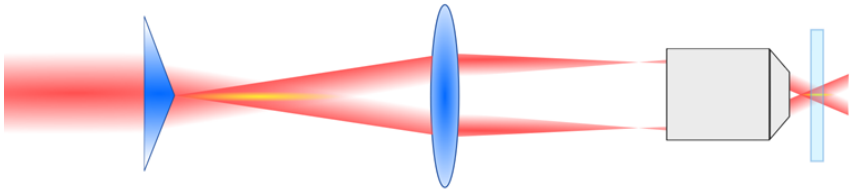

Fig. 2 Setup used to increase the cone angle of a primary Bessel beam. The lens and microscope objective are placed in a 2f-2fconfiguration to image the primary Bessel beam. Copyright Remi Meyer.

Recently, a new kind of architecture has been developed to reach Bessel zone lengths of several millimeters. A first version has been developed by Chebbi *et al* [26]. This has been recently improved in [27] to avoid any intermediate focusing. As shown in Fig. 3, the first two axicons are complementary and creates a wide annulus of light that is further focused using a very high angle axicon.

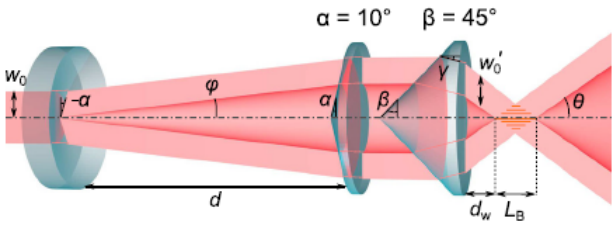

Fig. 3 Setup to generate extended Bessel beams with high cone angles and a long working distance (indicated as d_w). Reprinted figure with permission from [27].

The intensity over the optical axis of Bessel-Gauss beams varies smoothly. By controlling the diffraction efficiency of the phase mask applied by spatial light modulators or diffractive optical elements, it is possible to generate Bessel beams where the on-axis intensity is nearly constant over a segment, which is important for applications to laser nano-structuring [28, 29]. A new approach using geometrical phase optics, has been developed for the same purpose in reference [30].

1.2 Extended focal length and applications to surface structuring

Ultrafast laser ablation is characterized by a very marked threshold. Nano-structuring is made possible by adjusting the sample area over which the fluence exceeds the ablation threshold. Nanostructures can be processed with diameters even well below the wavelength [31]. For this application, the laser distribution must have strong

gradients. This is conventionally performed using tightly focused Gaussian beams, as shown in Fig. 4(a). However, in this case, the longitudinal positioning range over which the surface of the solid can be nano-structured is on the same order of magnitude as the diameter of the structures. This renders the sample positioning critical which is generally an obstacle to large area processing for real-life applications.

In this context, the quasi-arbitrary length of the Bessel zone allows fully lifting this constraint. A number of works have demonstrated surface nano-structuring using Bessel-Gauss beams, including processing of non-flat samples or opto-perforation of cells, which position is inherently difficult to control [18]. The sub-micron ablation of Indium Tin Oxide (ITO) has been demonstrated by Sahin [32] and Doan *et al* demonstrated the ablation of transparent conductive oxide through the substrate, so as to improve the final surface quality [33]. The extended Bessel zone allows for compensating flatness and thickness variation of the sample. The same property holds for higher order Bessel beams, used by Wetzel to process graphene [34] and holds more generally for all extended interference fields [35, 36]. Recently, the process has been extended to homogeneously write nano-ripples at the surface on a highly curved sample [37], as shown in Fig. 4(b).

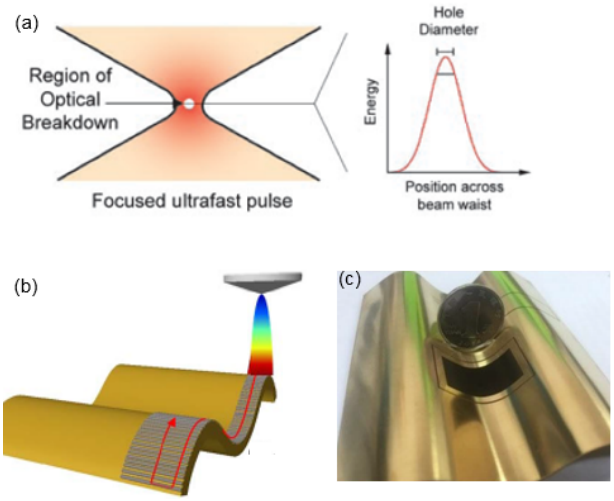

Fig. 4 (a) Optical breakdown can be induced on lateral dimension much smaller than the spot size, but it also implies that the longitudinal extent over which the sample surface is placed is restricted to the same order of magnitude [31], (b,c) The central lobe of diffraction-free Bessel beam provides a large longitudinal range where identical illumination conditions can be obtained. Li *et al* demonstrated homogeneous laser nanoprocessing on non-flat sample [37]. (a) Reprinted figure with permission from [31]; (b,c) Reprinted figure with permission from [37].

The longitudinal invariance of a Bessel beam is also useful to produce high aspect ratio microstructures inside metallic or dielectric materials by percussion drilling. Indeed, even when it is partially obstructed, the Bessel beam maintains its structure, obviously over a shorter length. Alexeev et al demonstrated that a Bessel

beam maintains a higher intensity over a longer length than Gaussian beams when propagating inside a deep channel made inside a metallic sample [38]. It is although noticeable that tapering occurs very frequently on most high aspect ratio structures in opaque materials [39]. In diamond, graphitization occurs very rapidly after few laser pulses, such that tapering also occurs when drilling trenches [40, 41].

Another important property of Bessel beams is that they are self-healing: after an obstacle, the intensity maximum reconstructs because of the conical flow of light. Nguyen *et al* have used this property, in addition to the extended Bessel zone, to create high aspect ratio microstructures in additive manufacturing. The presence of the powder only moderately effects the beam structure [42].

2 Non-diffracting beams for high aspect ratio nano-structuring the bulk of transparent materials

The most striking benefits with Bessel beams in terms of laser materials processing lies in the processing of transparent materials, particularly in a near-single burst illumination regime. In this section, we discuss the propagation of relatively high intensity pulses, from regimes where they are used for two-photon photopolymerization to regimes where the laser-deposited energy density is high enough to open a void inside the transparent solid. The related applications will be discussed in the next section.

2.1 Propagation in the bulk of transparent dielectrics and nano-plasma formation

When propagating inside a transparent dielectric, ultrashort pulses undergo the nonlinear self focusing Kerr effect, and, if the intensity is sufficiently high, an electron-hole plasma is generated. This plasma both partially absorbs and defocuses the pulse. These multiple effects are obviously highly nonlinear: the filamentation regime where all these effects are combined, is very difficult to predict and to scale. Gaussian beams in the filamentation regime undergo a strong spatial and spectral reshaping [43]. The physics of the nonlinear propagation of Bessel beams differs significantly from the one of Gaussian beams. It has been described in detail by Polesana *et al* [44].

In a pure Kerr medium, in absence of losses, an ultrafast Bessel beam undergoes reshaping by four wave mixing. Several new spatio-spectral components are generated: a wave parallel to the optical axis and a wave with the radial wavevector $\sqrt{2}k_r^0$ [45]. Engineering the spatial spectrum of the Bessel pulse can stabilize the beam [46, 47], but, with the perspective of laser structuring, most of the stabilization can come from nonlinear losses occurring within the central core. Porras *et al* demonstrated the existence of stationary solutions, *i.e.*, propagation-invariant, based

on a conical flow of light associated to nonlinear losses, even in presence of Kerr effect. These solutions can be seeded using Bessel beams. Noticeably, the stationary regime exists when both cone angle and nonlinear losses are sufficiently high. The non–stationary regime of the filamentation of Bessel beams can be associated to the periodic formation of plasma with applications to the imprinting of periodic marks inside fused silica [45].

When the cone angle is sufficiently high, the impact of Kerr effect becomes negligible. The length over which an optical ray crosses a high intensity region is limited to the about 1 µm, which implies that the accumulated Kerr phase is close to zero. In addition, when the cone angle is high enough, stabilization occurs from the high nonlinear losses due to nonlinear ionization and plasma absorption [44]. In this case, a plasma rod can be generated within the central core of the Bessel beam. The plasma density is highly homogeneous and the applications reviewed below take benefit of this homogeneity.

Garzillo and co-workers experimentally compared the propagation of femtosecond and picosecond pulses in BK7 glass [48]: the picosecond regime seemed to be more stable than the femtosecond one. In practice, picosecond pulses undergo less spectral reshaping and less plasma defocusing. A similar argument was raised by the group of R. Stoian (Univ. Lyon-Saint Etienne, France) who highlighted that the higher peak power of femtosecond pulses tend to enable ionization over a wider transverse distance than the picosecond ones as shown in Figure 5. The picosecond regime therefore seems therefore more favourable to a higher localization of energy deposition within the Bessel beam central lobe.

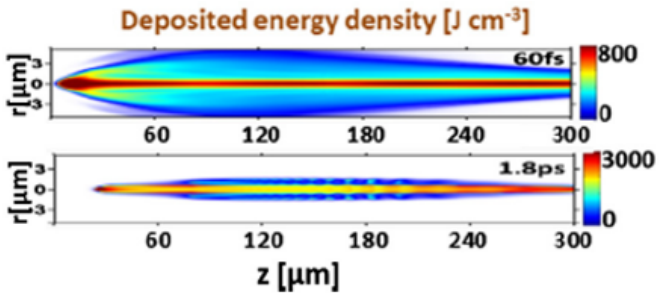

Fig. 5 Comparison of energy deposition by a Bessel beam wihin fused silica using nonlinear Schrödinger equation for a single pulse of duration 60fs pulse (top) and 1.8 ps (bottom). Reprinted figure with permission from [49].

It is worth noticing that these results are formulated on simulations based on paraxial nonlinear Schrödinger equation. It is an approximation to Maxwell's equations obtained after neglecting longitudinal components of the field and the plasma is treated as a static medium of permittivity fixed by Drude model [50]. This approach eliminates the possibility of modelling plasma waves. Although these approximations are extremely useful to model the filamentation dynamics inside solids [51, 43], they are no longer valid under strong focusing conditions to model the interaction

with nano-scaled plasmas. This is even more true when the plasma density reaches the critical density, at which the permittivity turns to zero. Beuton *et al* predicted with a full Maxwell code the possibility of reaching over-critical plasma densities [52]. The additional effect of resonance absorption has been very recently demonstrated to occur in these conditions for a femtosecond Bessel beam: most of the absorption is collisionless [53]. This is an effect which was not captured by the models described above and that will be discussed at the end of this section.

2.2 Link to the filamentation of Gaussian beams

The propagation of Bessel beams inside solid dielectrics has been popularized because it is a close cousin of the filamentation of Gaussian beams. More precisely, during the nonlinear filamentation process, Gaussian beams self-reshape into Bessel-like beams [54]. Filaments and Bessel beams in presence of nonlinear losses are both characterized by an intense central core, surrounded by an energy reservoir. Nonlinear stationary Bessel beams can be seen as the asymptotic structure of filamentation after a long propagation distance where the dynamics becomes stationary, *i.e.*, propagation-invariant.

To efficiently trigger filamentation, most authors use high power pulses or bursts of pulses either with moderate focusing to induce a dynamic reshaping by Kerr effect, or, more often for laser structuring applications, a relatively high focusing associated to spherical aberration [55, 56, 57]. Spherical aberration focuses the field components with the strongest radial wavevectors first, while the weakest radial wavevector components are focused at longer propagation distances. This way, a Gaussian beam with spherical aberration closely resembles to a Bessel beam (see Fig. 6 (left). Ahmed *et al* exploited this property by inserting a thick plate of fused silica between the focusing lens and the transparent workpiece where the filamentation had to be created [58] (Fig. 6(right)). This enables a high degree of control of the filamentation, very close to what be achieved using geometrical optics to control the position of the Bessel beam. Recently, Alimohammadian *et al* used conical phases in the Fourier space to strengthen the filamentation and to longitudinally shift the position of the filament inside transparent materials by several hundreds of micrometers [59, 60].

2.3 High aspect ratio index modification

Using a Bessel beam with moderately high fluence (typ. 10^{13} W.cm^{-2}), a sub-critical plasma is generated inside transparent dielectrics. This has been characterized for instance by Velpula *et al* using two-color time-resolved microscopy [61]. The plasma of excited free-electrons relax as heat or via self-trapping which induce structural rearrangements as described in [62] to yield positive or negative index modifications depending on the material and the relaxation pathway. This regime was used in early

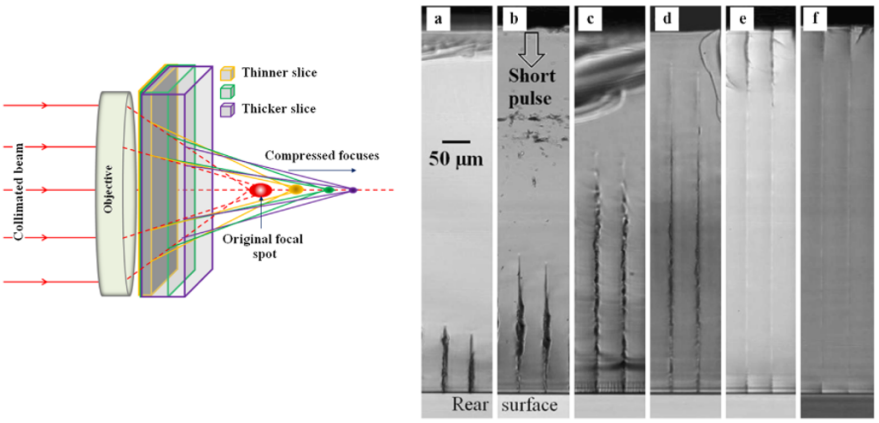

Fig. 6 (left) Concept of the spherical aberration induced by a thick glass slide inserted after the focusing objective (right) views of cleaved surfaces of the longest single shot voids fabricated with different inserted glass plate thickness (a) no glass, (b) 1 mm, (c) 2 mm, (d) 3 mm,(e) 5 mm, (f) 6 mm. Reprinted figure with permission from [58].

works to generate a homogeneous index modification inside glass [63, 64] by using low cone angles.

2.4 High aspect ratio nano-void formation

Single shot drilling

Interestingly, if the input pulse energy and the focusing of the Bessel beam are strong enough, a single laser pulse is enough to generate a high aspect ratio nano-void inside glass, which was first demonstrated in our group [8]; it is shown in Fig. 7. With Gaussian beams, void opening was also observed previously, but much stronger focusing is required, typically with numerical apertures close or above one [65, 66].

The filamentation regime where a Gaussian beam non-linearly self-transform to generate a relatively homogeneous nano-plasma, can also deposit sufficient energy density to open elongated nano-voids, for instance in PMMA [56], or glass [67, 59, 60].

We can remark here that this regime is significantly different from what can be generated using temporal Airy pulses, where it is the plasma dynamics that induces a spatial reshaping. This generates an elongated filament, typically on the order of 30 µm and a high aspect ratio channel close to the surface of glass [68, 69]. This regime is reviewed in detail in chapter 15.

The observation of these high aspect ratio voids with nanoscale diameter, under scanning electron microscopy (SEM) is particularly challenging. Several techniques have been developed throughout the years: initially, Bhuyan *et al* were mechanically

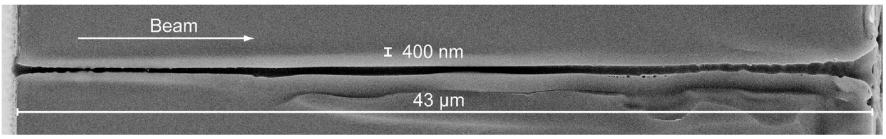

Fig. 7 High aspect ratio nanochannel generated by a single pulse of a Bessel beam with cone angle 11° in glass. Reprinted figure with permission from [8].

cleaving the channels. To increase the reliability of the imaging, Focused Ion Beam (FIB) milling was used later [70]: using the ion beam, a large cuvette is first drilled in the vicinity of the void, providing access to the SEM beam to image the vertical plane containing the longitudinal cross-section of the void. Then, a very fine approach, removing progressively the material by vertical layers of typically 40 nm, and intermediate imaging, allows imaging the nano-scale void with high resolution. Importantly, this process is overall very long ($\approx$ 1h per void), limited to depths of approximately 30 µm, and the void channel must be perfectly perpendicular to the sample surface such that the FIB beam milling is parallel to the high aspect ratio void. Very recently, Chen *et al* developed an efficient technique to overcome those difficulties: the drilling of void channel is repeated at different longitudinal positions inside the sample, then, fine polishing of the sample surface provides access to the transverse cross-section of the voids at different heights using SEM. A 3D reconstruction is then possible [71].

High aspect ratio void formation has been observed in a very large number of transparent materials: fused silica, different glasses, chalcogenide glasses, PMMA, ZnS [72] and even in materials as hard as sapphire [70]. The void opening requires a strong gradient of energy deposition, associated to relatively fast cooling. Importantly, the modification produced inside the transparent material is not always a void particularly at the highest energies. In this case, it is very often that irregular bubbles form in the position of the Bessel beam central core. This typically occurs when a relatively large diameter of material has been melt around the void. Depending on the material, the highest energies can be associated to the formation of an index modification on a large diameter. Figure 8 shows several types of modifications created in different materials with various parameters.

Influence of pulse duration

Figure 9 compares the modification created in sapphire for two different pulse durations under relatively strong focusing ($\theta = 26°$ in air). In the femtosecond case (top left), the void channel is free from apparent defects under SEM imaging, while the picosecond case (top right) shows a much wider heat affected zone and redeposited nanoparticles. In the latter case, it is apparent that the void opening was associated to a transient hot vapour phase where nanoparticles could nucleate. Void formation in the femtosecond case is still under debate as we will see below.

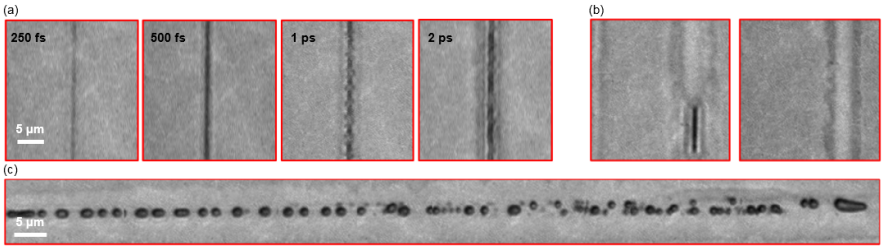

Fig. 8 (a) Different morphologies of material modification after single shot Bessel beam illumination with the same pulse energy with different pulse durations. (b) Modification inside Gorilla glass, for a 3 ps pulse, at two different positions inside the sample (c) Same as in (b) with three times higher pulse energy. Reprinted figure with permission from [73].

It is important to remark that high aspect ratio nanovoids can be created both using femtosecond or picosecond pulse durations, but, in the femtosecond regime, stronger focusing is needed (cone angle typically above 10° inside the solid). In this high focusing condition, voids could be opened using pulse durations down to 50 fs, where, conventionally, avalanche ionization cannot be triggered. This shows that the physics of the interaction, at least in the femtosecond regime, is not yet fully understood. In glass and fused silica, picosecond pulses generally yield modifications that are more visible under conventional microscopy: they are probably wider, and show a wider heat affected zone. Some modifications extend several micrometres away from the channel center (see for instance Figure 2 of reference [74]).

Bursts

As the benefit of the picosecond pulse duration is to reduce the peak power to increase the localization of the energy deposition inside the central core of the Bessel beam (see Fig. 5), it is also interesting to investigate the reduction of peak power by splitting the pulse into several sub-pulses. The result highly depends on the duration between the pulses.

In the void formation regime, our group has investigated the effect of splitting the femtosecond pulse in two equal sub-pulses, separated by durations between 0 to 500 ps [75]. Below a pulse separation of approximately 10 ps, the morphology and length of the void was varying shot-to-shot. But interestingly, above a pulse separation of 10 ps, the voids that were formed could have increased diameter in comparison with a single shot case, and smaller energies could give rise to smaller diameter voids. In this case, a diameter close to 100 nm could be reached.

Using absorption measurements, it was shown that the overall absorption was not increasing in comparison with the single pulse case. Therefore, the increase of drilling efficiency is due to an increased energy density deposited by the sequence of two pulses. The material after the first shot undergoes a progressive transformation on a scale of typically 10 ps: in this hot dense state, the material is highly absorbing.

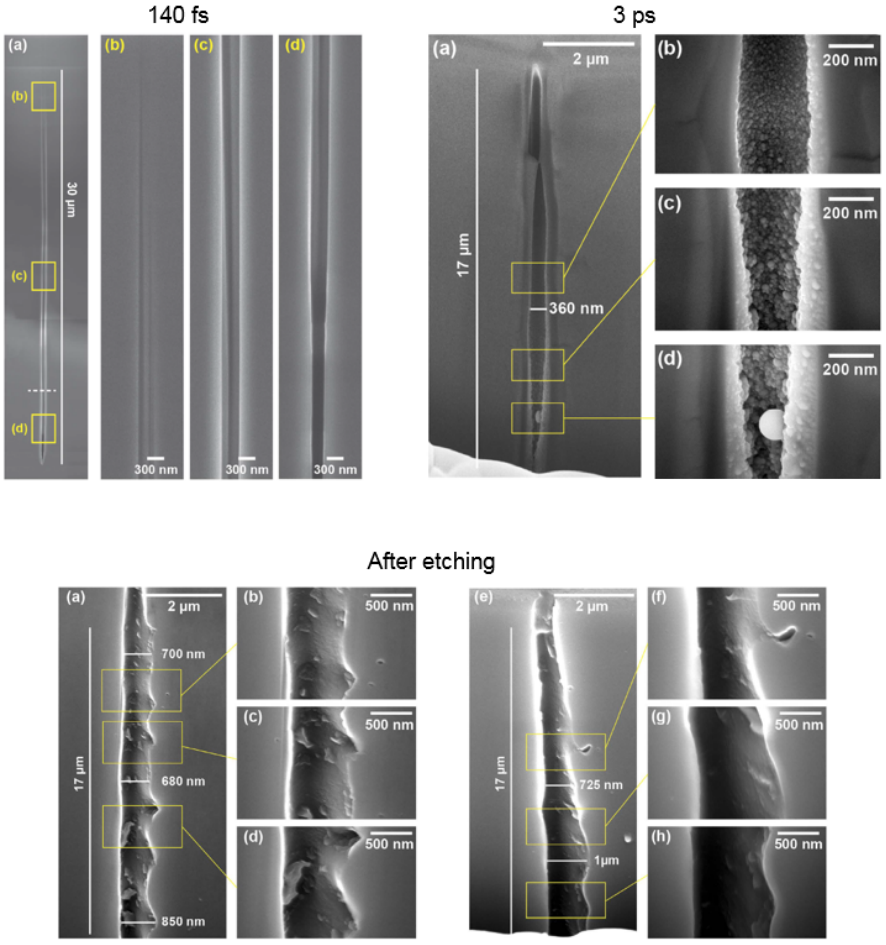

Fig. 9 High aspect ratio nano-voids generated in the bulk of sapphire in the single pulse regime using a Bessel beam with cone angle 14° in sapphire. (left column) pulse duration of 140 fs; (right column) pulse duration of 3 ps; (top row) SEM imaging after FIB milling; (bottom row) after HF etching of the FIB milled structures. The picosecond case shows a larger heat affected zone and cracks. Adapted figure with permission from [70].

This result matches the pump-probe measurements of Garcia-Lechuga at the surface of fused silica [76] as well as simulation results predicting the transformation of fused silica into warm dense matter when the laser deposited energy density reaches several MJ/kg [77, 78] as it is the case after the first pulse the Bessel beam configuration [75]. This state is long-living, probably more than several nanoseconds [79], which is why the enhancement of drilling efficiency is observed for bursts of pulses separated by up to several tens of ns as characterized by Kumkar *et al* [80, 81] and frequently used in the application of stealth dicing as we will see in the next section.

Depending on the exact geometrical configuration, some transient wave guiding effect has been observed, to increase the length of the modification. This is possible for relatively low cone angles, where the beam can be trapped into the waveguide created by the first pulse [82]. More generally, burst pulse configuration can benefit of the heat accumulation to create wider and stronger modifications. Although the burst configuration has been successfully used for stealth dicing, systematic comparisons of the diameter evolution with the burst parameters have still to be performed.

Pulse polarization

In fused silica and glass, no effect of the pulse polarization have been yet observed. Although it can slightly modify the ablation threshold because of the difference in nonlinear ionization cross-sections, the cross-sections of the channels are circular whatever the polarization. In contrast, in sapphire, voids generated using a linear polarization, in the femtosecond regime, have an elliptical transverse cross-section, oriented perpendicularly to the polarization direction [53]. The ellipticity can be used to control the formation of cracks [70]. In the picosecond regime, for pulse durations above 600 fs, high-power Bessel beams create cracks in several directions, which indicates that the void cross-section is circular [83].

Heat-affected zone

The formation of high aspect ratio voids fully enclosed in sapphire or glass demonstrates that part of the material is compressed around the void. In the case of sapphire, Rapp *et al* evaluated the compression ratio to ∼15% [70].

Recently, using FIB milling and chemical etching, Zhang *et al* characterized that, around the 290 nm diameter void channel drilled in fused silica with 4 ps pulses, the material is annealed over a diameter of ~ 2 µm, corresponding to the Bessel beam core and cracks develop only at a further distance, typically 2 µm (see Fig. 10) [84]. These micro-cracks are key for the application to stealth-dicing mentioned in section 3.

2.5 Physics of energy deposition and void opening. Current challenges

The physics of the energy deposition process is particularly difficult to characterize because of the nanometric value of the characteristic scales involved. A very interesting discussion on experimental flaws is provided in section II.B of reference [85]. This field has been very active in the recent years, with several techniques that were developed to characterize the nonlinear pulse propagation and energy deposition inside transparent dielectrics. Bergner *et al* developed a pump-probe microscopy technique to image the filamentation of 6 ps pulses [86]. Their technique was capa-

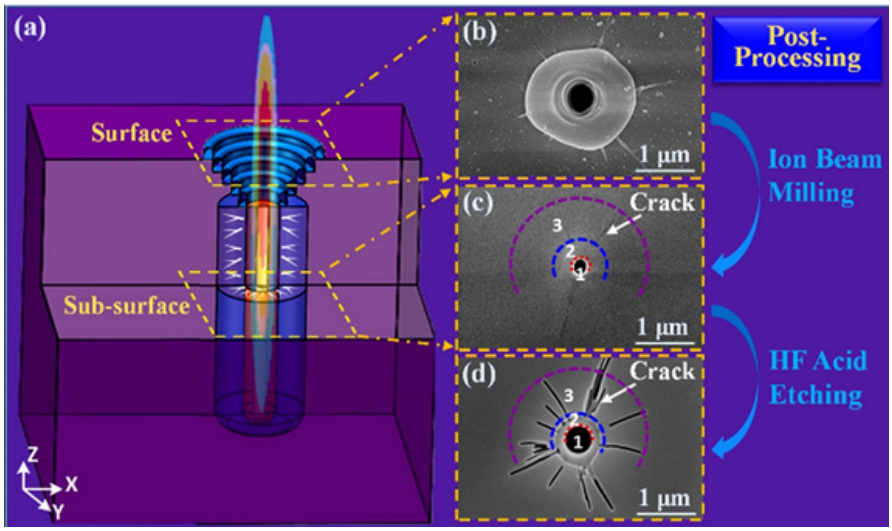

Fig. 10 SEM imaging of a void transverse cross section inside fused silica. in (c), the void is inside the red dotted line (1), the annealed region (2) is enclosed in the blue circle and the third region with cracks is within the purple circle. (d) shows the same area after HF etching to reveal the cracks. Reprinted figure with permission from [84].

ble to retrieve the local index of refraction. This technique was particularly efficient to show the impact of Kerr effect ahead of the focal region, the buildup of the plasma which particularly extends in time toward the laser source. One can notice also that their results demonstrate that the region where the maximal temperature is reached, around the Gaussian beam focus, is maintained hot during several nanoseconds at least, in agreement with the results mentioned in Section 2.4. This is the region where the strongest material modification is observed. The spatial resolution of this technique is unfortunately not enough to characterize the formation of nanovoids.

As it was mentioned earlier in Section 2.1, the energy deposition during the pulse propagation has not yet been completely modeled. The computationally-efficient models using nonlinear Schrödinger equation cannot describe the detail of the physics occurring when submicron plasma is generated. Using first-principles particle-in-cell numerical simulations that are based on solving Maxwell's equations together with particles trajectories [87, 88], our group has recently demonstrated that a very important absorption mechanism was collisionless, which is conventionally very difficult to capture using simulations [53]. This collisionless absorption is a combination of two effects. The first is resonance absorption: when a p-polarized pulse impinges on a plasma ramp, the pulse is deviated at the so-called turning point where the density reaches $\rho = \rho_c \cos i$, where ρ_c is the critical density and i the incidence angle on the plasma. (Note that for Bessel beams, the turning point shifts away from the optical axis when the cone angle $\theta = \pi/2 - i$ is decreased). The evanescent field created from the turning point tunnels to the critical density point where it can resonantly excite electrostatic plasma waves –also named Langmuir or longitudinal waves in

the literature – [88]. If the turning point and critical point are close enough, the conversion efficiency can be very important, typically up to 60% [89]. The second effect is the damping of the plasma wave by several plasma wave-particle interaction processes such as Landau damping and transit acceleration. These interactions are collisionless processes [88]. Overall, in conditions close to the regime of nanovoid formation with femtosecond pulses (e.g. [8] and [70]), our simulations demonstrated that over 90% of the absorption is collisionless. This shows that most of the literature models still have to be adapted to fully interpret the dynamics of plasma build-up and laser-plasma interaction during the pulse propagation.

After the energy has been deposited in form of an electron-hole plasma inside the dielectric, a number of relaxation processes take place. They highly depend on the energy density that was deposited by the laser pulse. For relatively low ionization degree, the free electron relaxation involves phonon excitation, generation of self-trapped excitons, themselves relaxing in the form of structural deformations. However, for the case of void opening, it is more likely that high energy densities are involved. When the ionization percentage typically reaches 20% (see the case of silicon in reference [90]), lattice disordering can occur at ultrafast scales [91], yielding bandgap shrinking, as observed recently in fused silica by Winkler *et al* [92].

A number of experiments corroborate the fact that a fast transition to a hot state arise approximately in the picosecond scale after the laser pulse. Somayaji *et al* reported the absence of trapping at the sub-picosecond scale in fused silica [79], while the trapping of free carriers occurs within 150 fs in the case of weak ionization [93]. The same authors also reported photoluminescence and spectrally-resolved photoluminescence at the ns-scale, demonstrating a phase on the order of 5000 K, well above the boiling point of silica and close to its critical point [94]. This is consistent with the observation of a transformation at ps-scale toward a regime of warm dense matter by Hoyo *et al* [75] as well with the refractive index measurements on the filamentation of picosecond Gaussian beams of reference [86] Heat diffusion occurs during several hundreds of nanoseconds, in association with potential phase changes.

Two scenarii were discussed for the actual opening of the void structure. References [95] and [65], considering the voids formed by tightly focused Gaussian beams, first hypothesized a mechanism where the pressure reached by the plasma creates a micro-explosion that compresses the solid material around. Numerical simulations based on elasto-plastic modelling including the equation of state of fused silica showed the feasibility of this mechanism for an ultrafast Bessel pulse. In this mechanism, the void would open on timescales of several hundreds of picoseconds [96, 52].

Bhuyan *et al* used phase contrast microscopy to characterize the dynamics of plasma and void formation using femtosecond and picosecond pulses, shaped as Bessel beams [97, 98]. The measurements shown in Fig. 11 seem to show that the void opening takes place between 1 to several milliseconds after the laser pulse. A second mechanism has therefore been suggested : cavitation could occur within an over-heated liquid [98]. Similar dynamics is observed using picosecond pulses

[79]. However, the experimental setup cannot distinguish the radial distribution of the index of refraction. It is possible that the high temperature reached around the microexplosion site, with a high positive refractive index contribution, could mask part of the process at early times. For now, the differences observed between the femtosecond and picosecond regime in terms of void morphology (Fig. 9) are not yet fully explained. More experimental and simulation work is required to fully answer this question. We finally remark that, in the case warm dense matter is actually generated in the relaxation of the plasma, this state of matter is still challenging to model and is not described by the Drude model [99].

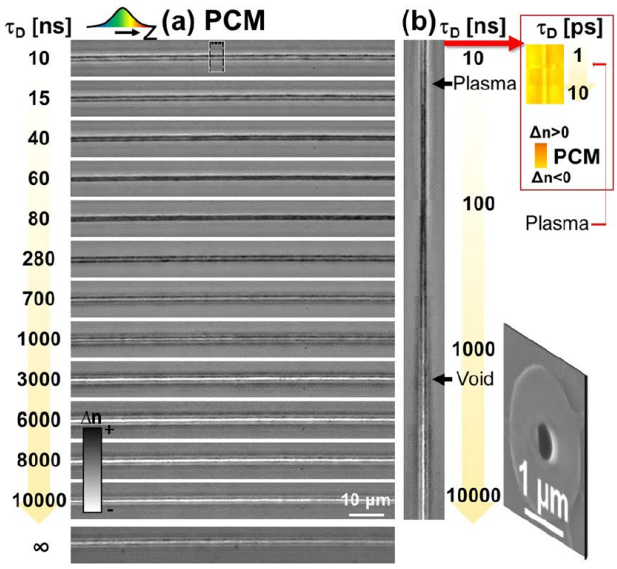

Fig. 11 (a) Time-resolved sequence of phase contrast imaging corresponding to the appearance of a high-aspect ratio void inside fused silica after illumination by a chirped pulse of 5 ps duration (propagation from left to right); (b) Concatenation of cross-cuts of the images of (a) to show the evolution of the dynamics in time (log-scale); The inset shows the dynamics at early times in identical conditions, from ref. [98]. Reprinted figure with permission from [79].

3 Applications to high-aspect ratio nano-structuring

Ultrafast non-diffracting Bessel beams have been successfully used in a number of applications where high aspect ratio micro- or nano-structures are required.

3.1 Two-photon photopolymerization

Two-photon photopolymerization is a powerful fabrication technique to produce almost arbitrary shaped components and tools, scaling from millimeters to sub-micrometer, useful to a wide range of applications [100, 101, 102]. However, point-by-point irradiation is a very slow process. Zeroth and higher-order Bessel beams have been used to parallelize the process and produce two or three-dimensional structures by avoiding the translation of the beam in one or more directions, see [2] and references therein, [103, 104].

3.2 Index modifications and gratings

At low fluence, the long, subcritical plasma channels created by ultrafast pulses shaped as Bessel beams in the single or multishot regime, induce a local modification of the index of refraction. These modifications are highly homogeneous and can be positive or negative depending on the material [105]. Glass photosensitivity can also be used to control the laser-induced modifications [106]. High aspect ratio smooth modifications were successfully used to generate volumetric Bragg gratings in PMMA, PDMS or fused silica by a number of different groups [107, 108, 109, 110]. Because of the width of the heat affected zone, the modifications cannot be processed arbitrary close to each other and the laser inscription often imposes operating on higher-order of the Bragg grating. Still, the reflectivity of these gratings could reach up to 90% [110]. Reference [111] demonstrates extremely efficient pass- and stop-bands nearly with transmission of respectively nearly 100% and 0% .

The stress field induced within the material by the laser-induced modifications can interestingly be shaped to generate engineered optical anisotropies. In this context, Bessel beam provide a mean to create optically thick modifications [112].

High aspect ratio modifications in fused silica and glass can be etched using hydrofluoric acid (HF) or potassium hydroxide (KOH), so as to serve for micro-fabrication purposes. Several works have been performed to increase the etching efficiency, particularly using double pulse illumination to benefit from the localized absorption of self-trapped excitons [113, 114].

We finally remark in this section that in a near ablation regime, using a high number of pulses, self-organized nanovoids appear. They are shaped as lamellas oriented perpendicular to the polarization. Bessel beams allow for generating such gratings over extended volumes, as shown and modelled by Rudenko *et al* [115, 116]. They find applications in laser fabrication of photonic components with space-varying anisotropy.

3.3 Laser welding

Joining materials is required in almost all fabrication fields and scales. Because it is highly flexible and contact-free, laser welding is obviously highly attractive. Ultrashort laser pulses allow for welding glass and, more generally transparent materials between themselves as well as glass with another material. The ultrashort character of the pulses provide, via nonlinear ionization, the ability to control in 3 dimensions the position of the heat source. However, welding requires generally a relatively large volume of molten material to fill the small gap between the parts to be joined. Filamentation and Bessel beams are ideally positioned to locally fuse the transparent material over an elongated volume and relax in addition, the constraint on surface positioning. The idea has been very early developed by Tamaki *et al* and further developed by several groups [117, 118, 119]. The use of actual Bessel beams is more recent [120]. Importantly, the joined parts can become as strong as the bulk material itself. The illumination strategy, including heat accumulation using long burst, is an important factor to release the constraints and improve the stiffness of the weld parts [119]. Hecker *et al* highlighted the role of the conical structure of the Bessel beam to maintain a homogeneous illumination during melting [121].

3.4 Nano-voids for photonics

To build in-line spectrometers, is necessary to have the means to extract a fraction of the light traveling inside optical waveguides. High aspect ratio nano voids can be used as very efficient scattering centers for this purpose. The high index contrast provided by the void highly increases the efficiency for the light extraction in comparison with a more conventional index modification on the order of 10^{-2}. This has been nicely demonstrated to build spectrometers for astro-photonics, operating in the mid-infrared window, with waveguides and light extraction written inside a chalcogenide glass [122, 123] as illustrated in Fig. 12. Using a similar approach, reference [124] demonstrates very strong Bragg resonances for Bragg filters in the telecommunications window. The group of P. Herman, Toronto, corrected the aberration due to the curvature of optical fibers to laser-inscribe a chirped array of high aspect ratio nano voids on a relatively short extent of the waveguide, not only to extract light out of the waveguide, but also to focus the output coupled light directly onto a camera without a lens. In this case, the nanovoids were also enlarged using chemical etching [125].

A second application of nano-voids is the fabrication of photonic crystals. However, as already mentioned, it is difficult to process voids very close to each other because of the diameter of the heat affected zone and because the previously drilled channels impact on the Bessel beam propagation. However, for this application, it is not necessary that the aspect ratio is extremely high. Liu *et al* have engineered the Bessel beam length to reduce the aspect ratio and produce relatively compact photonic crystals [126, 127]. In addition, at the air-solid interface, the voids often

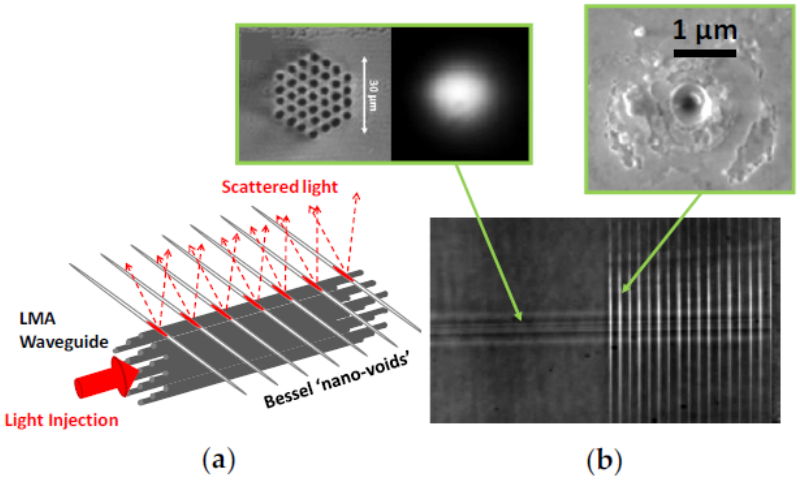

Fig. 12 Concept (left) and images of a photonic crystal waveguide structure inside chalcogenide glass (top images). The Bessel-induced nanovoids are used as scattering centers to couple light out of the waveguide. Reprinted figure with permission from [123].

show a trumpet-like profile. A non-homogeneous diameter is obviously detrimental for photonic crystals. The same authors have polished the surface of the sample after laser processing to obtain highly homogeneous nano-structures [127].

3.5 Drilling and cutting of glass and sapphire

High-speed cutting and drilling of glass is essential for a large number of mass fabrication applications, particularly in the field of microelectronics and consumer electronics. The need is to drill and/or separate glass sheets with a thickness comprised between some tens to several hundred micrometres. The resistance of glass should be preserved, it should be free of chipping with limited number of defects in the vicinity of the cut surface.

Drilling

It has been recently demonstrated that Bessel beams allow for cutting the whole thickness of glass slide, by translating the Bessel beam onto a trajectory while the beam is positioned such as to cross both front and exit surfaces. With this strategy, it was possible to obtain non-tapered, vertical walls for cutting of contours and opening, in transparent materials, circular holes of several tens of micrometers in diameter. An example of diamond drilling is presented in Fig. 13. Noticeably, the burst regime, although improving the ablation rate, is not always the best option

to obtain the highest quality structures [128, 129, 130]. An improvement of the ablation efficiency can be obtained using double pulses with a typical delay of 50 ps, which corresponds to the lifetime of self-trapped excitons [114] (in this case, the pulse energy is usually lower than the one needed to open a void in single shot). An alternative approach to linear beam shaping is to produce, by nonlinear pulse propagation into a water film flowing on a workpiece, a filament, which is then used to process the workpiece. Water also contributes to material removal [131].

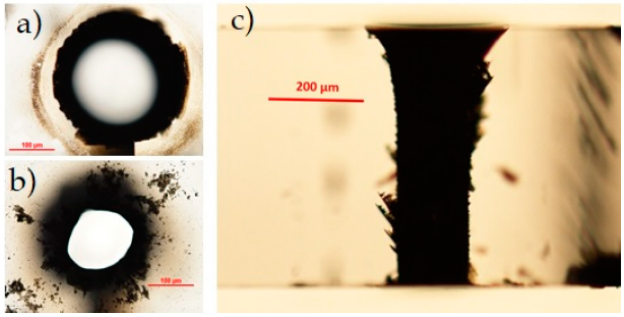

Fig. 13 Through-via drilled inside 500 µm thick diamond, using 100 writing circles. (a) top, (b) bottom and (c) lateral views. Reprinted figure with permission from [130].

To increase the ablation removal rate while drilling high aspect ratio craters in glass, Ito *et al* have used the superposition of a femtosecond laser filament to a continuous-wave beam at 1064 nm wavelength. The free-electrons generated inside the filament absorb the continuous laser light efficiently. The high amount of energy absorbed over a cylinder inside glass opens an ablation crater with a diameter of 10 µm and a length of ∼130 µm in 40 ms [132, 133].

Transparent material separation without ablation. Stealth Dicing

Stealth dicing of glass is probably one of the most important commercial application of ultrafast lasers in the last decade. Although the material to separate is at millimeter thickness scale, it is the control of laser-induced nanometric modifications that enable a drastically new regime of separation. Stealth dicing was initially developed to cut silicon wafers at high speed [134]. It consists of generating a plane of defects within the depth of a brittle material to cut, and in a second step, of applying a stress such that a fracture propagates through the defects and cleaves the workpiece. In the initial technology, the laser was a nanosecond infrared source, and the modifications in silicon were extending over some tens of micrometers.

A similar technique was developed by Ahmed *et al* for glass separation with micrometric resolution [136, 58]. In this case, the modifications were based on the filamentation of ultrashort pulses. Figure 14 compares different types of modifications tested to reach high-speed and high-quality cutting. A typical separation

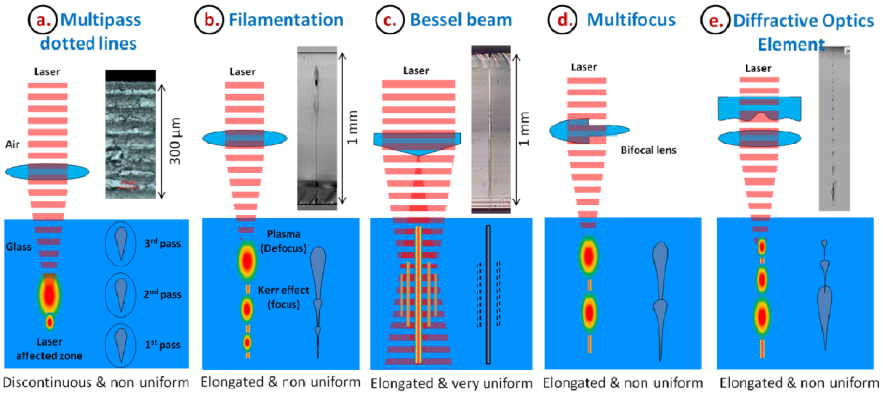

Fig. 14 Different strategies for ultrafast laser inscription of modifications inside glass for stealth-dicing. Reprinted figure with permission from [135].

between the high aspect ratio voids is ~5-25 µm, such that a laser source with repetition rate of several 100's kHz allows for processing glass at a speed on the order of 1 m/s. Apart from speed, the benefit is the quasi-absence of dust particles since it is not really an ablative process. The kerf is zero and, in optimal conditions, the method is free from chipping.

First implementations of Bessel beams in this field were performed by Tsai [137] and Bhuyan [138]. The main benefit is to produce a highly homogeneous stress distribution along the material thickness, which is crucial to maintain a high cut quality for tempered glass [138]. In this reference, the authors demonstrated from mechanical cleaving that the optimal beam position was fully inside the sample and used single pulses with a pulse duration of 11 ps. Cutting was achieved at a speed of 270 mm/s.

Overall, the cutting can be along straight or curved paths [80] and the surface quality is conventionally relatively rough (typ. between 0.5 µm to several µm). It is highly linked to the extension of internal cracks [67] and therefore to the illumination parameters as described in [135]. Particularly, the use of bursts and thermal load can benefit to the cleaving operation [80] but requires fine adjustment for instance using a dash-line strategy [135].

As for the second step, the cleaving operation, several approaches were used: most research groups used mechanical flexure, whereas CO_2 laser provides highly repeatable conditions [67, 139]; we can also note that tempered glass is internally stressed by the chemical treatment such that it self-cleaves.

Although the stealth dicing technology has promptly emerged and attracted the interest of a large number of research groups and companies, only few publications quantitatively compared the different techniques. Li *et al* compared filamentation-based cleaving of glass to laser surface scribing and to combinations of filamentation and V-groove scribing, against a number of criteria: cleaving guidance, reproducibility, breaking force, morphology of the cut surface and flexural strength of the cut

parts. Using a single pulse filamentation, the assistance of a V-groove was found to improve the cutting quality. Overall, the best results were found for a burst-mode filamentation, when the filament is formed fully inside the 1 mm -thick glass sample. The authors reported sub-micron roughness of the cleaved facets, with the nicest edges and a flexural strength nearly equal to the pristine reference material [140]. Dudutis *et al* quantitatively compared Bessel-beam based stealth dicing using sub-picosecond pulses with more conventional glass cutting techniques such as laser-based rear side machining, mechanical scribe-and-cleave, water jet cutting or diamond-saw cutting [141]. Their analysis also involved a number of criteria, including residual stress. The Bessel beam approach provided the results with the less residual surface cracks and chipping. Yet a the flexural strength of the cut samples is less than for conventional rear-side machining, we note that the regime of pulse duration and energy used here with the Bessel beam, creates a large heat affected zone and cracks extending over several tens of micrometers, which are very likely fragilizing the cut material. Shorter pulse durations tend to minimize the damaged region. We can remark that the procedure used to apply the stress that separates the samples appears to be an important parameter although the field is yet lacking of published studies.

Thick glass cutting

Most of previously mentioned work dealt with the cutting of relatively thin flat glass sheets, with thickness ranging from 30 µm to approximately 2 mm, because the typical Bessel zone or filament length is on the order of 200-700 µm. Cutting of multi-mm thick glass requires other strategies. A first approach is to generate multiple modification surfaces, on top of each other to cover most of the glass thickness in multiple passes. This approach obviously decreases the overall process throughput and requires a fine alignment of the planes written on top of each other, which needs high repeatability translation stages.

A second approach is to extend the Bessel zone length to multi-millimeter scale so as to enable cutting using a single laser pass. Extending the beam length using the same cone angle imposes to increase the pulse energy in the same ratio as the length increase. For multi-mm-long ranges, the burst energy should be on the order of 1 mJ. It is difficult to use such energy in the conventional telescopic setup used to magnify the cone angle (see Section 1.1) mostly because of the risk of optical damage to the second lens. Indeed, as the Bessel zone extends, its Fourier-transform is thinner, with a much higher energy than for the processing of thin samples. To avoid the use of the 2f-2f setup, high apex angle axicons were used to shape the ultrafast laser beam. .

To increase the working distance to several millimeters, the 3-axicon shaping technique of reference [26], was implemented to produce 8 mm-long modifications in glass [142]. (We remark that in ref. [143], a single axicon is used, with obvious limitation onthe working distance, but mJ pulses used enabled cutting 8 mm glass in single pass.) The setup was slightly improved using a pair of negative and positive axicons to avoid any intermediate hot spots or focusing [27] (see Section 1). With

this approach, extremely thick glass, up to 1 cm thick glass could be cleaved using the stealth dicing technique [27]. Noticeably, the aspect ratio of the nano-voids, using the same geometry, has been scaled from 100:1 in [8] to 30 000:1 in [27]. Very thick glass cutting opens new opportunities to reduce costs for window-glass processing in a context where better insulating windows are required to limit our carbon footprint.

4 Perspectives

Thick and thin glass processing using diffraction-free Bessel beams has been very active in the recent years. Even more recently, a number of new orientations have attracted attention. It was realized that shaping the central lobe of the Bessel beam could enhance the performances of stealth dicing. The stealth dicing technique has also been widened to curved glass cutting. New strategies are being developed to cut glass with curved surface in a single pass and finally, the family of Bessel beams has been generalized to create almost arbitrary transverse cross-sections that propagate preserving the conical flow and longitudinal invariance.

4.1 Crack formation

Micro-crack formation seems to be the mechanism allowing material separation where the stress-induced fracture propagates through the laser-induced crack network. The transient stress and crack propagation imaging has been reported in [144, 145]. Cracks with a transverse extension of several tens of micrometers can be produced using high-energy pulses, particularly when using relatively long pulse duration. Increasing the crack extent allows for increasing the channel to channel distance and, while this increases the surface roughness, straightforwardly improves the process speed.

In sapphire, cracks can be generated following the crystal axes. Rapp *et al* demonstrated that, using approximately 10 times the energy needed to produce a nanochannel in single shot, cracks extending over $\sim$ 20 µm were generated in a star-shape following the three axes of the hexagonal lattice. Interestingly, below a pulse duration of $\sim$ 600 fs, only a single crack is generated, perpendicular to the polarization axis. This can be understood from the elliptical transverse shape of the nano-void formed in the femtosecond regime (see Section 2.5). Polarization could then be used to control the crack direction, although a non-trivial coupling exists with the stress induced by formerly drilled nanochannels. These results were also confirmed in reference [146], in which cutting of sapphire along a curved path is demonstrated at 500 mm/s (see Fig. 15).

In glass, the transverse cross section of the channels does not show any ellipticity. This can be controlled using a specific beam shape, for instance by producing an elliptical Bessel beam, formed by filtering part of the intensity ring distribution in the

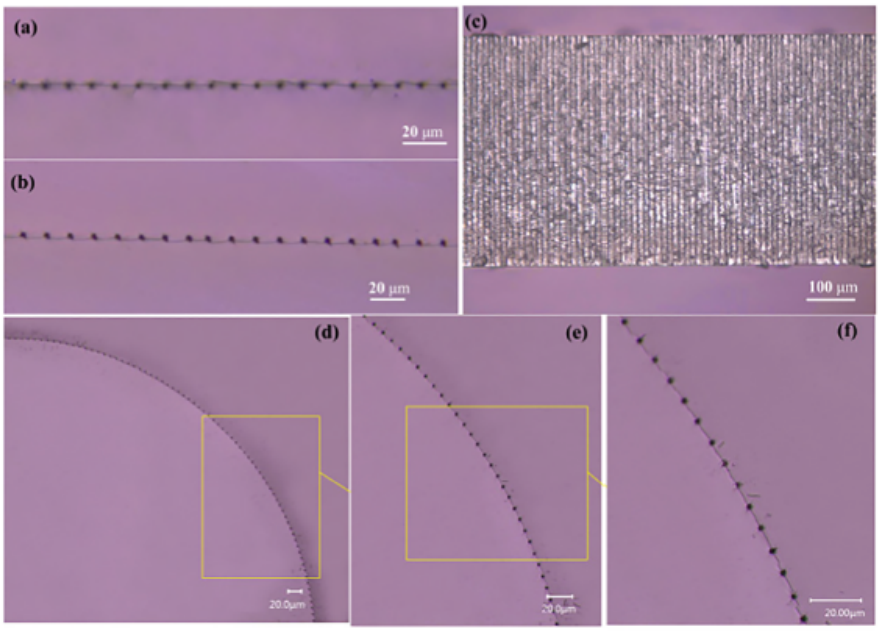

Fig. 15 Control of the formation of cracks after Bessel beam illumination. The cutting speed is 0.5 m/s. Reprinted figure with permission from [146].

Fourier space [147] or by using more complex beam shaping approaches [148, 149] or simply using imperfect axicons, or an axicon with a tilt [21, 150, 151]. The elliptical cross section of the channels increases the stress along the major axis of the ellipse. This improves the cleavability of the material and the flexural strength of the cut material [152]. Another similar approach using multiple cavities has been suggested and modelled in reference [153].

Another way of controlling the crack formation and improving the process throughput is the use of a dash-line strategy where groups of channels are processed and a crack joins the groups during material separation. This strategy improves guiding the overall fracture, particularly for the separation of materials cut along curved paths [135].

4.2 Aberration correction for non-flat glass cutting

The applications of glass cutting are by far not limited to flat glass neither vertical cutting. Glass vertically cut at 90° from its surface can undergo chipping or breaking when handled because of stress accumulation at the corners. However, the beam inclination that is necessary to create beveled edges, induces a strong beam distorsion, as can be observed from Fig. 16 (middle left). The subsequent intensity drop within

the beam prevents nanochannel drilling. Jenne *et al* compensated the aberration due to the inclined glass surface using a phase mask computed with a decomposition of the aberration on Zernike polynomials [154]. Successful cutting with 30° tilt angle is shown in Fig.16 (right). A more precise aberration correction was developed in reference [139], where the aberration is computed by inverse propagation. In this reference, the phase mask is additionally engineered to produce an elliptical Bessel beam.

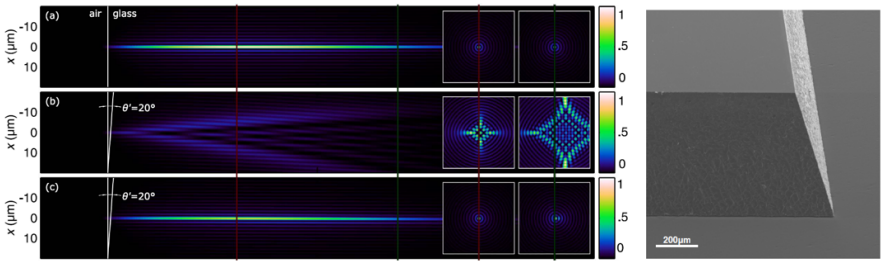

Fig. 16 (left) Simulation of Bessel beam intensity distribution inside glass: (a) if the glass surface is normal to the Beam axis, (b) if the surface is tilted by 20 °, (c) same as (b) but the Bessel beam is pre-corrected. (right) example of glass cutting with a tilt of 30 ° with respect to the normal. Reprinted figure with permission from [154].

A similar problem arises to cut curved surfaces such as glass tubes for ampoules or syringes. Flamm *et al* applied a quadratic phase compensation to preserve the shape of the Bessel beam inside a curved glass article. Figure 17 compares the beam intensity distribution produced within glass without and with the aberration correction. Obviously, the correction is dependent on the curvature of the article [155].

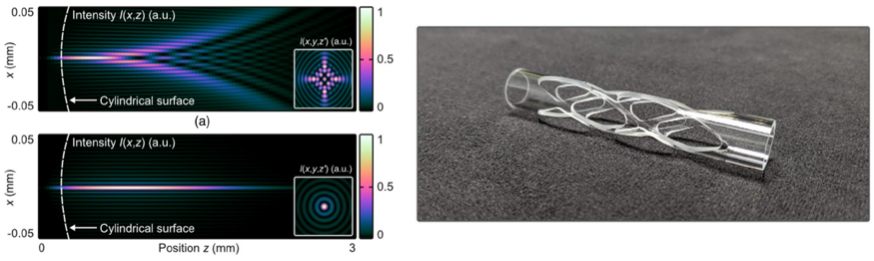

Fig. 17 (left) Simulation of Bessel beam intensity distribution inside curved glass, before (top) and after correction (bottom). (right) Complex contour cutting from a glass tube. Etching is used after laser illumination to enable material removal. Reprinted figure with permission from [155].

The cut parts of the tube shown in Fig. 17 have been removed using laser illumination with the corrected Bessel beam and chemical etching. This overall demonstrates the usefulness and flexibility of laser structuring using nondiffracting Bessel beams.

4.3 Laser Processing of curved structures

We discuss here the application to edge chamfering that is necessary for glass handling and reducing the stress accumulation within the corners, as mentioned in the above section 4.2. Instead of the three passes at three different angles that are necessary to cut and chamfer glass in a bull-nose shape, it would be desirable to have a process performing this operation in a single step. A fully curved profile would even more reduce the stress confinement due to sharp angles. In this context, other classes of extended beams, *i.e.*,accelerating beams, and in more general, beams with a curvature, can offer new opportunities.

Self-accelerating beams are beams which produce an interference pattern that laterally shift along a curve during propagation. A first version, the "Airy beam" was produced using a third order phase and an optical Fourier transformation [156]. It was early used to produce curved plasmas channels in air [157, 158]. By recognizing that accelerating beams are caustics, it is in fact possible to largely extend the self-acceleration property to arbitrary curved trajectories, that can even extend to the non-paraxial regime [159, 160, 161, 162, 163, 164].

First applications to curved laser micromachining were developed by Mathis *et al* where accelerating beams were used for edge polishing and curved trench opening [163, 165] and to inscribe a curved damage inside glass [161]. A challenging issue in the field is the generation of curvatures with large radius. This requires very large extents of the third order phase applied in the Fourier plane as well as optics with large pupils: the beams developed by Mathis *et al* could be curved only over a distance of typically 50 to 70 µm while reaching a tilt of $\pm \sim 45°$, see Fig. 18 (left). Recently, using a similar apporach, Sohr *et al* demonstrated curved modifications of 700 µm glass that could be etched, with a maximal tilt of $\sim 18°$, as shown in Fig. 18 (right) [166].

To circumvent the above-mentioned difficulty of phase extent to create an accelerating beam with large maximal tilt to process glass with thickness of several hundreds of micrometers to millimeters, a new strategy was developed in [167]. The concept, as shown in Fig. 19, is to generate a series of focii positioned on a curved trajectory. Very large tilt angles can be reached as can be seen in Fig. 19 (right).

4.4 Bessel-like beams and applications

Most of the works discussed up to here were based on zeroth-order Bessel beams. However, it is easy to understand that higher order Bessel beams, or other beam shapes could offer interesting perspectives in the field of laser micro-nano-machining.

Jukna *et al* demonstrated that higher order Bessel beams can sustain – if the cone angle is sufficiently high – the same propagation- invariant regime as the one generated by zeroth-order Bessel beams [168]. Higher-order Bessel beams have been tested by several groups for laser processing. However, a key aspect is that at the high power necessary to induce material modification, the cone angle generally used can

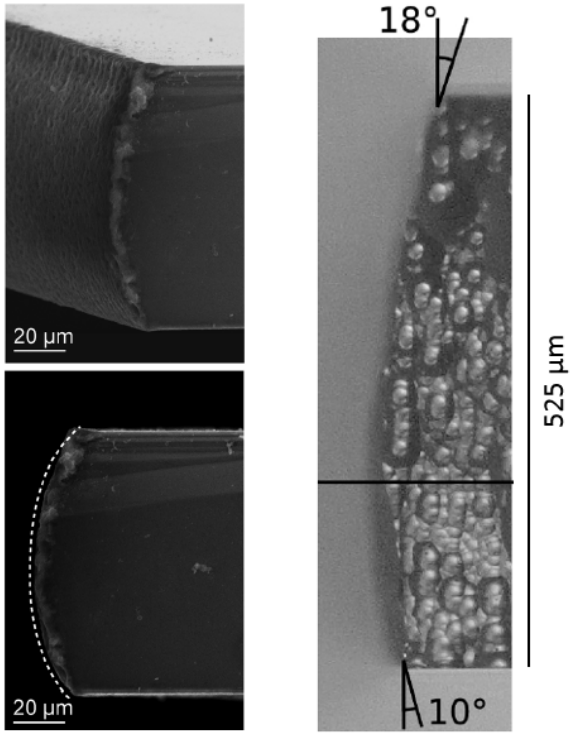

Fig. 18 (left) Curved edge processing of 50 µm thick silicon using an accelerating beam.Reprinted figure with permission from [165]; (right) Two-step curved edge processing in glass : laser illumination using an accelerating beam is used before chemical etching to enable material separation. Reprinted and adapted figure with permission from [166].

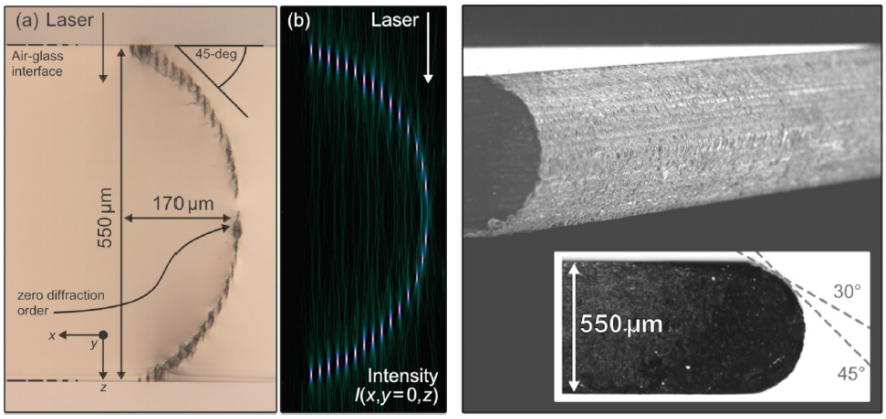

Fig. 19 Curved edge processing using a series of focii distributed over a half-circle. Material separation is obtained after chemical etching. Reprinted figure with permission from [167].

be insufficient to prevent nonlinear modulation instability. It tends to split the main intensity ring [169]. As shown in [170], the main ring of the higher-order Bessel can split into multiple hot-spots during the propagation. Jedkrkiewicz *et al* reported single-shot induced tubular modifications in glass using higher order Bessel beams in the picosecond regime [171]. In the femtosecond regime, modifications are visible only at the surface. In reference [172], azimuthal and radial polarizations of a first order Bessel beam have been compared in the context of picosecond laser crack formation inside glass. It was shown the most prominent effect is in fact the intensity asymmetries of the beam.

A new class of Bessel-like beams has been introduced by Jenne, Flamm *et al* with a generalization of the azimuthal phase applied. The phase of an *n*th-order Bessel beam is, in radial coordinates(r, ϕ):

$$\Psi(r, \phi) = \frac{2\pi}{\lambda} \sin \theta r + n\phi \tag{3}$$

This generates a beam with a transverse intensity profile close to $|J_n(r)|^2$ function. The first term is responsible for the conical structure of the beam while the second determines the transverse position of the intensity maxima, since they are the points of constructive interference. The concept introduced by Jenne and Flamm is to modify the second term, following [149, 148]:

$$\Psi(r, \phi) = \frac{2\pi}{\lambda} \sin \theta r + \Theta(\phi) \tag{4}$$

where Θ is an arbitrary function. With this approach, the group developed beam shapes that can efficiently control the formation of well-oriented extended cracks. The use of asymmetrically-shaped central lobe of Bessel beam [149] confirms the results of Meyer *et al* [152].

Figure 20 demonstrates that Bessel-like shaping opens a very large number of possibilities to engineer the stress distribution inside glass, obviously not limited to glass cleaving applications.

Other approaches have also been used to engineer Bessel beams while preserving their non-diffracting properties, such as superpositions of laterally shifted Bessel vortices [173], superpositions of vortices [174], or the synthesis of non-diffracting Mathieu and Weber beams [175]. Using superimposed vortex orders, Yu *et al* reduced the intensity of the sidelobes which was successfully applied to surface nanostructuring with reduced limitation on the fluence in the central peak, as shown in Fig. 21 [176].

Bessel-like beams have also benefited to the field of two-photon polymerization: Yang *et al* reported fabrication of complex tubular structures [177] as shown in Fig. 22, Arita *et al* created twisted microfibers [178].

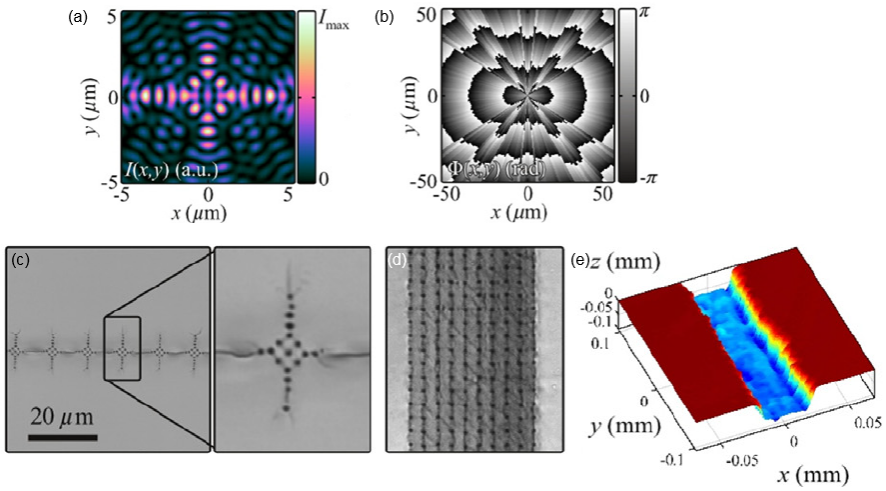

Fig. 20 (a) Cross section of a Bessel-like beam generated using the phase mask shown in (b). (c) SEM view of a series of ultrafast laser induced material modifications and cracks using the beam shape (a). (d) After scanning the beam over a series of lines, a square array of cracks and channels is created. (e) shows the profile of a trench after chemical etching of the sample shown in (d). Reprinted figure with permission from [155].

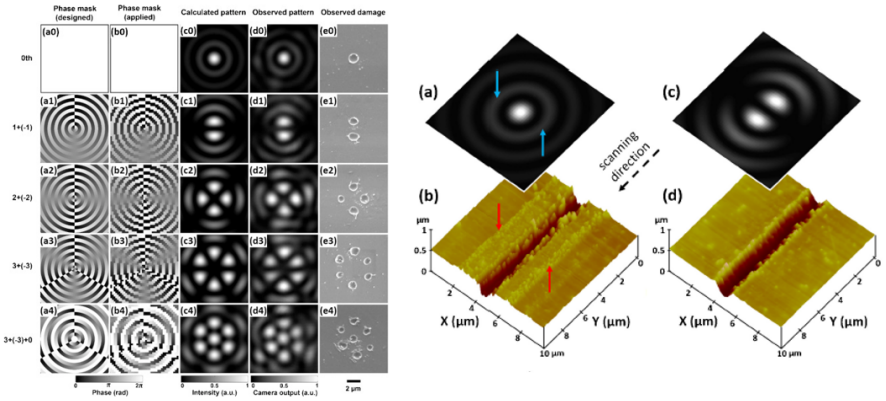

Fig. 21 (left) Superpositions of different Bessel beams leads to multiple spots and can be used to process material surface; (right) Trench nanomachining using an engineered Bessel-like beam can reduce the damage produced by side lobes. Reprinted figure with permission from [176].

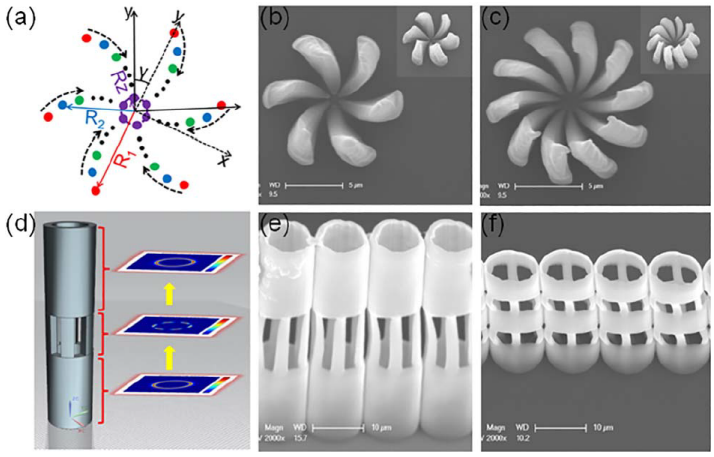

Fig. 22 (top row) Illumination concept and result of the two-photon polymerization. Scale bars are 5 µm. (bottom row) Concept of the fabrication process using the shaped beams and results. Scale bars are 10 µm. Reprinted figure with permission from [177].

Conclusion

As a conclusion, ultrafast laser beam shaping as quasi-diffraction-free Bessel beams that propagate in a conical flow, has enabled the development of drastically new laser nanostructuring applications, down to the extreme regime of 100 nm laser structuring and extremely high aspect ratio up to 30 000 to 1. The strength of the approach is that these extreme scales are also very well adapted for real-life technological applications. The very long focal region of Bessel beams releases the constraint on ultra-precise sample positioning when nanostructuring, non-flat surfaces can be processed. Inside solids, the laser beam shaping enables the generation of extended index modification, photopolymerization, or void formation with applications in photonics or to high-speed thin or thick glass cutting. We have also reviewed recent new directions of the field where new beam shapes are being developed , maintaining the conical flow property, but where the transverse intensity distribution is engineered to control targeted effects with enhanced transverse directionality. The recent generalization of Bessel beams and the development of non-diffracting caustics [179] open a new toolbox to control matter at extreme scales and extreme regimes with ultrafast laser pulses.

It is no doubt that next generation of very high power, kilowatt class lasers, will offer new opportunities for further developments since the extended focus of Bessel and Bessel-like beams require more energy and higher average power [180]. On a fundamental side, the nanometric scale of the laser-induced plasmas inside dielectrics still represents a challenge for the laser-matter interaction in this regime but recent results make us oversee that extreme states can be reached using these beam shapes with both fundamental and technological impact. Warm dense matter

can be generated over extremely long distances using only a tabletop laser, in contrast with much more complex high energy sources currently used. On the technological aspects, the extreme pressures and temperatures reached within the materials over lengths at centimeter-scale can offer also very interesting perspectives in terms of new material synthesis [181].

Acknowledgements FC acknowledges the financial supports of: European Research Council (ERC) 682032-PULSAR, Region Bourgogne-Franche-Comte and Agence Nationale de la Recherche (EQUIPEX+ SMARTLIGHT platform ANR-21-ESRE-0040), I-SITE BFC project (contract ANR-15-IDEX-0003), and the EIPHI Graduate School ANR-17-EURE-0002.

References

1. J. Durnin, J. J. Miceli, and J. H. Eberly. Diffraction-free beams. *Phys. Rev. Lett.*, 58(15):1499–1501, apr 1987.
2. M. Duocastella and C.B. Arnold. Bessel and annular beams for materials processing. *Laser & Photonics Reviews*, 6(5):607–621, jan 2012.
3. F. Courvoisier, R. Stoian, and A. Couairon. Ultrafast laser micro- and nano-processing with nondiffracting and curved beams. *Optics Laser Technology*, 80:125–137, June 2016.
4. Razvan Stoian, Manoj K. Bhuyan, Guodong Zhang, Guanghua Cheng, Remy Meyer, and Francois Courvoisier. Ultrafast bessel beams: advanced tools for laser materials processing. *Advanced Optical Technologies*, 7(3):165–174, 2018.
5. Razvan Stoian. Volume photoinscription of glasses: three-dimensional micro- and nanostructuring with ultrashort laser pulses. *Applied Physics A: Materials Science and Processing*, 126, 6 2020.
6. Francois Courvoisier. Ultrafast laser micro-nano structuring of transparent materials with high aspect ratio. In *Handbook of Laser Micro- and Nano-Engineering*, pages 1–37. Springer International Publishing, 2020.
7. V. Jarutis, R. Paškauskas, and A. Stabinis. Focusing of laguerre–Gaussian beams by axicon. *Optics Communications*, 184(1-4):105–112, oct 2000.
8. M. K. Bhuyan, F. Courvoisier, P.-A. Lacourt, M. Jacquot, L. Furfaro, M. J. Withford, and J. M. Dudley. High aspect ratio taper-free microchannel fabrication using femtosecond Bessel beams. *Opt. Express*, 18(2):566, 2010.
9. John H. McLeod. The axicon: A new type of optical element. *Journal of the Optical Society of America*, 44(8):592, 1954.
10. L. Froehly, M. Jacquot, P. A. Lacourt, J. M. Dudley, and F. Courvoisier. Spatiotemporal structure of femtosecond Bessel beams from spatial light modulators. *Journal of the Optical Society of America A*, 31(4):790, 2014.
11. P.A. Brandão and D.G. Pires. Transmission and reflection of vector Bessel beams through an interface between dielectrics. *Physics Letters A*, 381(8):813–816, feb 2017.
12. Narupon Chattrapiban, Elizabeth A. Rogers, David Cofield, III Wendell T. Hill, and Rajarshi Roy. Generation of nondiffracting Bessel beams by use of a spatial light modulator. *Optics Letters*, 28(22):2183, 2003.
13. Antti Vasara, Jari Turunen, and Ari T. Friberg. Realization of general nondiffracting beams with computer-generated holograms. *Journal of the Optical Society of America A*, 6(11):1748, 1989.
14. Jun Amako, Daisuke Sawaki, and Eiichi Fujii. Microstructuring transparent materials by use of nondiffracting ultrashort pulse beams generated by diffractive optics. *Journal of the Optical Society of America B*, 20(12):2562, 2003.

15. S. N. Khonina, V. V. Kotlyar, R. V. Skidanov, V. A. Soifer, K. Jefimovs, J. Simonen, and J. Turunen. Rotation of microparticles with Bessel beams generated by diffractive elements. *Journal of Modern Optics*, 51(14):2167–2184, sep 2004.
16. R. Grunwald, U. Neumann, V. Kebbel, H.-J. Kühn, K. Mann, U. Leinhos, H. Mischke, and D. Wulff-Molder. Vacuum-ultraviolet beam array generation by flat micro-optical structures. *Optics Letters*, 29(9):977, may 2004.
17. Thierry Grosjean, Said Sadat Saleh, Miguel Angel Suarez, Idriss Abdoulkader Ibrahim, Vincent Piquerey, Daniel Charraut, and Patrick Sandoz. Fiber microaxicons fabricated by a polishing technique for the generation of Bessel-like beams. *Appl. Opt.*, 46(33):8061, 2007.
18. X. Tsampoula, V. Garceés-Chavez, M. Comrie, D. J. Stevenson, B. Agate, C. T. A. Brown, F. Gunn-Moore, and K. Dholakia. Femtosecond cellular transfection using a nondiffracting light beam. *Appl. Phys. Lett.*, 91(5):053902, 2007.
19. Selcuk Akturk, Bing Zhou, Michel Franco, Arnaud Couairon, and Andre Mysyrowicz. Generation of long plasma channels in air by focusing ultrashort laser pulses with an axicon. *Optics Communications*, 282(1):129–134, jan 2009.
20. Pauline Boucher, Jesus Del Hoyo, Cyril Billet, Olivier Pinel, Guillaume Labroille, and François Courvoisier. Generation of high conical angle Bessel–Gauss beams with reflective axicons. *Applied Optics*, 57(23):6725, aug 2018.
21. Juozas Dudutis, Paulius GeČys, and Gediminas RaČiukaitis. Non-ideal axicon-generated Bessel beam application for intra-volume glass modification. *Optics Express*, 24:28433, 12 2016.
22. Oto Brzobohatý, Tomáš Cižmár, and Pavel Zemánek. High quality quasi-Bessel beam generated by round-tip axicon. *Opt. Express*, 16(17):12688, 2008.
23. Tomáš Čižmár and Kishan Dholakia. Tunable Bessel light modes: engineering the axial propagation. *Opt. Express*, 17(18):15558, 2009.
24. Simon Schwarz, Gian-Luca Roth, Stefan Rung, Cemal Esen, and Ralf Hellmann. Fabrication and evaluation of negative axicons for ultrashort pulsed laser applications. *Optics Express*, 28:26207, 8 2020.
25. Simon Schwarz, Stefan Rung, Cemal Esen, and Ralf Hellmann. Rapid fabrication of precise glass axicon arrays by an all laser-based manufacturing technology. *Journal of Laser Applications*, 32:012001, 2 2020.
26. Brahim Chebbi, Sergey Minko, Nezar Al-Akwaa, and Ilya Golub. Remote control of extended depth of field focusing. *Optics Communications*, 283(9):1678–1683, 2010.
27. R. Meyer, L. Froehly, R. Giust, J. Del Hoyo, L. Furfaro, C. Billet, and F. Courvoisier. Extremely high-aspect-ratio ultrafast bessel beam generation and stealth dicing of multi-millimeter thick glass. *Applied Physics Letters*, 114(20):201105, 2019.
28. Ismail Ouadghiri-Idrissi, Remo Giust, Luc Froehly, Maxime Jacquot, Luca Furfaro, John M. Dudley, and Francois Courvoisier. Arbitrary shaping of on-axis amplitude of femtosecond bessel beams with a single phase-only spatial light modulator. 24(11):11495–11504.
29. Raghu Dharmavarapu, Shanti Bhattacharya, and Saulius Juodkazis. Diffractive optics for axial intensity shaping of Bessel beams. *Journal of Optics (United Kingdom)*, 20, 7 2018.
30. Pavel Gotovski, Paulius Šlevas, Ernestas Nacius, Vytautas Jukna, Sergej Orlov, Justas Baltrukonis, Orestas Ulčinas, and Titas Gertus. Formation of optical needles by pancharatnam-berry phase element for laser-induced modifications in transparent materials. page 69. SPIE-Intl Soc Optical Eng, 3 2020.
31. A. P. Joglekar, H. h. Liu, E. Meyhofer, G. Mourou, and A. J. Hunt. Optics at critical intensity: Applications to nanomorphing. *Proceedings of the National Academy of Sciences*, 101(16):5856–5861, 2004.
32. Ramazan Sahin and Ismail Kabacelik. Nanostructuring of ito thin films through femtosecond laser ablation. *Applied Physics A: Materials Science and Processing*, 122, 4 2016.
33. Due Hong Doan, Ryoichi Iida, Byunggi Kim, Isao Satoh, and Kazuyoshi Fushinobu. Bessel beam laser-scribing of thin film silicon solar cells by ns pulsed laser. *Journal of Thermal Science and Technology*, 11, 3 2016.

34. Benjamin Wetzel, Chen Xie, Pierre-Ambroise Lacourt, John M. Dudley, and Francois Courvoisier. Femtosecond laser fabrication of micro and nano-disks in single layer graphene using vortex bessel beams. *Appl. Phys. Lett.*, 103(24):241111, 2013.
35. B. Voisiat, M. Gedvilas, S. Indrišiūnas, and G. Račiukaitis. Picosecond-laser 4-beam-interference ablation as a flexible tool for thin film microstructuring. *Physics Procedia*, 12:116–124, 2011.
36. Sabri Alamri and Andrés Fabián Lasagni. Development of a general model for direct laser interference patterning of polymers. *Optics Express*, 25(9):9603, 2017.
37. Xiaowei Li, Zhijie Xu, Lan Jiang, Yaoming Shi, Andong Wang, Lingling Huang, and Qunshuo Wei. Creating a three-dimensional surface with antireflective properties by using femtosecond-laser Bessel-beam-assisted thermal oxidation. *Optics Letters*, 45:2989, 6 2020.
38. I. Alexeev, K.-H. Leitz, A. Otto, and M. Schmidt. Application of Bessel beams for ultrafast laser volume structuring of non transparent media. *Physics Procedia*, 5:533–540, 2010.
39. Y. Matsuoka, Y. Kizuka, and T. Inoue. The characteristics of laser micro drilling using a bessel beam. *Appl. Phys. A*, 84(4):423–430, 2006.
40. Ottavia Jedrkiewicz, Sanjeev Kumar, Belén Sotillo, Monica Bollani, Andrea Chiappini, Maurizio Ferrari, Roberta Ramponi, Paolo Di Trapani, and Shane M. Eaton. Pulsed Bessel beam-induced microchannels on a diamond surface for versatile microfluidic and sensing applications. *Optical Materials Express*, 7:1962, 6 2017.
41. Sanjeev Kumar, Shane M. Eaton, Monica Bollani, Belén Sotillo, Andrea Chiappini, Maurizio Ferrari, Roberta Ramponi, Paolo Di Trapani, and Ottavia Jedrkiewicz. Laser surface structuring of diamond with ultrashort Bessel beams. *Scientific Reports*, 8, 12 2018.
42. Huu Dat Nguyen, Xxx Sedao, Cyril Mauclair, Guillaume Bidron, Nicolas Faure, Enrique Moreno, Jean Philippe Colombier, and Razvan Stoian. Non-diffractive Bessel beams for ultrafast laser scanning platform and proof-of-concept side-wall polishing of additively manufactured parts. *Micromachines*, 11, 11 2020.
43. A Couairon and A Mysyrowicz. Femtosecond filamentation in transparent media. *Physics Reports*, 441(2-4):47–189, mar 2007.
44. P. Polesana, M. Franco, A. Couairon, D. Faccio, and P. Di Trapani. Filamentation in Kerr media from pulsed Bessel beams. *Phys. Rev. A*, 77(4):043814, apr 2008.
45. Eugenijus Gaizauskas, Egidijus Vanagas, Vygandas Jarutis, Saulius Juodkazis, Vygantas Mizeikis, and Hiroaki Misawa. Discrete damage traces from filamentation of Gauss-Bessel pulses. *Optics Letters*, 31(1):80, 2006.
46. Ismail Ouadghiri-Idrissi, John M. Dudley, and Francois Courvoisier. Controlling nonlinear instabilities in Bessel beams through longitudinal intensity shaping. *Optics Letters*, 42(19):3785, sep 2017.
47. Ismail Ouadghiri-Idrissi, John M. Dudley, and Francois Courvoisier. Control of spatial four-wave-mixing efficiency in bessel beams using longitudinal intensity shaping. *Physical Review A*, 100(4):043804, 2019-10.
48. Valerio Garzillo, Vytautas Jukna, Arnaud Couairon, Robertas Grigutis, Paolo Di Trapani, and Ottavia Jedrkiewicz. Optimization of laser energy deposition for single-shot high aspect-ratio microstructuring of thick BK7 glass. *Journal of Applied Physics*, 120, 7 2016.
49. Praveen Kumar Velpula, Manoj Kumar Bhuyan, Cyril Mauclair, Jean-Philippe Colombier, and Razvan Stoian. Role of free carriers excited by ultrafast bessel beams for submicron structuring applications. *Optical Engineering*, 53(7):076108, 2014.
50. L. Sudrie, A. Couairon, M. Franco, B. Lamouroux, B. Prade, S. Tzortzakis, and A. Mysyrowicz. Femtosecond laser-induced damage and filamentary propagation in fused silica. *Phys. Rev. Lett.*, 89(18):4135, oct 2002.
51. S. Tzortzakis, L. Sudrie, M. Franco, B. Prade, A. Mysyrowicz, A. Couairon, and L. Bergé. Self-guided propagation of ultrashort IR laser pulses in fused silica. *Physical Review Letters*, 87(21), nov 2001.
52. R. Beuton, B. Chimier, P. Quinoman, P. González Alaiza de Martínez, R. Nuter, and G. Duchateau. Numerical studies of dielectric material modifications by a femtosecond Bessel–Gauss laser beam. *Applied Physics A: Materials Science and Processing*, 127, 5 2021.

53. Kazem Ardaneh, Remi Meyer, Mostafa Hassan, Remo Giust, Chen Xie, Benoit Morel, Ismail Ouadghiri-Idrissi, Luca Furfaro, Luc Froehly, Arnaud Couairon, Guy Bonnaud, and Francois Courvoisier. A new route to high energy density inside the bulk of transparent materials. *arXiv*, page 2109.00803, 2021.
54. D. Faccio, M. Clerici, A. Averchi, O. Jedrkiewicz, S. Tzortzakis, D. Papazoglou, F. Bragheri, L. Tartara, A. Trita, S. Henin, I. Cristiani, A. Couairon, and P. Di Trapani. Kerr-induced spontaneous bessel beam formation in the regime of strong two-photon absorption. *Optics Express*, 16(11):8213, 2008.
55. Le Luo, Dangling Wang, Chengde Li, Hongbing Jiang, Hong Yang, and Qihuang Gong. Formation of diversiform microstructures in wide-bandgap materials by tight-focusing femtosecond laser pulses. *Journal of Optics A: Pure and Applied Optics*, 4(1):105–110, dec 2001.
56. S. Sowa, W. Watanabe, J. Nishii, and K. Itoh. Filamentary cavity formation in poly(methyl methacrylate) by single femtosecond pulse. *Applied Physics A*, 81(8):1587–1590, nov 2005.
57. Juan Song, Xinshun Wang, Xiao Hu, Ye Dai, Jianrong Qiu, Ya Cheng, and Zhizhan Xu. Formation mechanism of self-organized voids in dielectrics induced by tightly focused femtosecond laser pulses. *Applied Physics Letters*, 92(9):092904, mar 2008.
58. Farid Ahmed, M. Shamim Ahsan, Man Seop Lee, and Martin B. G. Jun. Near-field modification of femtosecond laser beam to enhance single-shot pulse filamentation in glass medium. *Applied Physics A*, 114(4):1161–1165, apr 2013.
59. Ehsan Alimohammadian, Erden Ertorer, Erick Mejia Uzeda, Jianzhao Li, and Peter R. Herman. Inhibition and enhancement of linear and nonlinear optical effects by conical phase front shaping for femtosecond laser material processing. *Scientific Reports*, 10:21528, 12 2020.
60. Ehsan Alimohammadian, Erden Ertorer, and Peter R. Herman. Conical phase front and aberration beam shaping for manipulating femtosecond laser chemical etching. *Optical Materials Express*, 11:2432, 8 2021.
61. P. K. Velpula, M. K. Bhuyan, F. Courvoisier, H. Zhang, J. P. Colombier, and R. Stoian. Spatio-temporal dynamics in nondiffractive Bessel ultrafast laser nanoscale volume structuring. *Laser & Photonics Reviews*, 10(2):230–244, mar 2016.
62. Razvan Stoian, Manoj Kumar Bhuyan, Anton Rudenko, Jean Philippe Colombier, and Guanghua Cheng. High-resolution material structuring using ultrafast laser non-diffractive beams. *Advances in Physics: X*, 4, 1 2019.
63. Andrius Marcinkevicius, Saulius Juodkazis, Shigeki Matsuo, Vygantas Mizeikis, and Hiroaki Misawa. Application of Bessel beams for microfabrication of dielectrics by femtosecond laser. *Japanese Journal of Applied Physics*, 40(Part 2, No. 11A):L1197–L1199, nov 2001.
64. Véronique Zambon, Nathalie McCarthy, and Michel Piché. Fabrication of photonic devices directly written in glass using ultrafast bessel beams. In Réal Vallée, Michel Piché, Peter Mascher, Pavel Cheben, Daniel Côté, Sophie LaRochelle, Henry P. Schriemer, Jacques Albert, and Tsuneyuki Ozaki, editors, *Photonics North 2008*. SPIE, 2008.
65. S. Juodkazis, K. Nishimura, S. Tanaka, H. Misawa, E. G. Gamaly, B. Luther-Davies, L. Hallo, P. Nicolai, and V. T. Tikhonchuk. Laser-induced microexplosion confined in the bulk of a sapphire crystal: Evidence of multimegabar pressures. *Phys. Rev. Lett.*, 96(16):166101, apr 2006.
66. Saulius Juodkazis, Hiroaki Misawa, Tomohiro Hashimoto, Eugene G. Gamaly, and Barry Luther-Davies. Laser-induced microexplosion confined in a bulk of silica: Formation of nanovoids. *Applied Physics Letters*, 88(20):201909, may 2006.
67. Ferdinand Werr, Alexander Veber, Martin Brehl, Michael Bergler, Dirk Werner, Urs Eppelt, Ludger Müllers, and Dominique de Ligny. Surface probing of ultra-short-pulse laser filament cut window glass and the impact on the separation behavior. *Advanced Engineering Materials*, 22, 9 2020.
68. Nadine Götte, Thomas Winkler, Tamara Meinl, Thomas Kusserow, Bastian Zielinski, Cristian Sarpe, Arne Senftleben, Hartmut Hillmer, and Thomas Baumert. Temporal airy pulses for controlled high aspect ratio nanomachining of dielectrics. *Optica*, 3(4):389, 2016-04.

69. S.W. Winkler, I.M. Burakov, R. Stoian, N.M. Bulgakova, A. Husakou, A. Mermillod-Blondin, A. Rosenfeld, D. Ashkenasi, and I.V. Hertel. Transient response of dielectric materials exposed to ultrafast laser radiation. *Appl. Phys. A*, 84(4):413–422, jul 2006.
70. L. Rapp, R. Meyer, R. Giust, L. Furfaro, M. Jacquot, P. A. Lacourt, J. M. Dudley, and F. Courvoisier. High aspect ratio micro-explosions in the bulk of sapphire generated by femtosecond Bessel beams. *Scientific Reports*, 6(1), sep 2016.
71. Tianqu Chen, Guodong Zhang, Yishan Wang, Xuelong Li, Razvan Stoian, and Guanghua Cheng. Reconstructing of embedded high-aspect-ratio nano-voids generated by ultrafast laser Bessel beams. *Micromachines*, 11, 7 2020.
72. Gai Yan Chang, Yu Heng Wang, and Guang Hua Cheng. Writing nanopores on a zns crystal with ultrafast Bessel beams. *Chinese Optics*, 14:213–225, 1 2021.
73. Christian Vetter, Remo Giust, Luca Furfaro, Cyril Billet, Luc Froehly, and Francois Courvoisier. High aspect ratio structuring of glass with ultrafast bessel beams. *Materials*, 14(22):6749, 2021.
74. M. Lamperti, V. Jukna, O. Jedrkiewicz, P. Di Trapani, R. Stoian, T. E. Itina, C. Xie, F. Courvoisier, and A. Couairon. Invited article: Filamentary deposition of laser energy in glasses with Bessel beams. *APL Photonics*, 3, 12 2018.
75. Jesus del Hoyo, Remi Meyer, Luca Furfaro, and Francois Courvoisier. Nanoscale confinement of energy deposition in glass by double ultrafast bessel pulses. *Nanophotonics*, 10(3):1089–1097, 2020.
76. M. Garcia-Lechuga, L. Haahr-Lillevang, J. Siegel, P. Balling, S. Guizard, and J. Solis. Simultaneous time-space resolved reflectivity and interferometric measurements of dielectrics excited with femtosecond laser pulses. *Phys. Rev. B*, 95:214114, 2017.
77. A. Denoeud, A. Benuzzi-Mounaix, A. Ravasio, F. Dorchies, P. M. Leguay, J. Gaudin, F. Guyot, E. Brambrink, M. Koenig, S. Le Pape, and S. Mazevet. Metallization of warm dense SiO2 studied by XANES spectroscopy. *Phys. Rev. Lett.*, 113(11), 2014.
78. K. Engelhorn, V. Recoules, B. I. Cho, B. Barbrel, S. Mazevet, D. M. Krol, R. W. Falcone, and P. A. Heimann. Electronic structure of warm dense silicon dioxide. *Phys. Rev. B*, 91(21), 2015.
79. Madhura Somayaji, Manoj K. Bhuyan, Florent Bourquard, Praveen K. Velpula, Ciro D'Amico, Jean Philippe Colombier, and Razvan Stoian. Multiscale electronic and thermomechanical dynamics in ultrafast nanoscale laser structuring of bulk fused silica. *Scientific Reports*, 10, 12 2020.
80. M. Kumkar, L. Bauer, S. Russ, M. Wendel, J. Kleiner, D. Grossmann, K. Bergner, and S. Nolte. Comparison of different processes for separation of glass and crystals using ultrashort pulsed lasers. In Alexander Heisterkamp, Peter R. Herman, Michel Meunier, and Stefan Nolte, editors, *Frontiers in Ultrafast Optics: Biomedical, Scientific, and Industrial Applications XIV*. SPIE, 2014.
81. K. Mishchik, R. Beuton, O. Dematteo Caulier, S. Skupin, B. Chimier, G. Duchateau, B. Chassagne, R. Kling, C. Hönninger, E. Mottay, and J. Lopez. Improved laser glass cutting by spatio-temporal control of energy deposition using bursts of femtosecond pulses. *Optics Express*, 25:33271, 12 2017.
82. Samira Karimelahi, Ladan Abolghasemi, and Peter R. Herman. Rapid micromachining of high aspect ratio holes in fused silica glass by high repetition rate picosecond laser. *Applied Physics A*, 114(1):91–111, nov 2013.
83. L. Rapp, R. Meyer, L. Furfaro, C. Billet, R. Giust, and F. Courvoisier. High speed cleaving of crystals with ultrafast Bessel beams. *Optics Express*, 25(8):9312, apr 2017.
84. Guodong Zhang, Razvan Stoian, Rui Lou, Tianqu Chen, Guangying Li, Xu Wang, Yan Pan, Pengfei Wu, Jiang Wang, and Guanghua Cheng. Thermal and mechanical limitations to processing resolution in volume non-diffractive ultrafast laser structuring. *Applied Surface Science*, 570, 12 2021.
85. Nadezhda M. Bulgakova, Vladimir P. Zhukov, Svetlana V. Sonina, and Yuri P. Meshcheryakov. Modification of transparent materials with ultrashort laser pulses: What is energetically and mechanically meaningful? *Journal of Applied Physics*, 118(23):233108, dec 2015.

86. K. Bergner, B. Seyfarth, K. A. Lammers, T. Ullsperger, S. Döring, M. Heinrich, M. Kumkar, D. Flamm, A. Tünnermann, and S. Nolte. Spatio-temporal analysis of glass volume processing using ultrashort laser pulses. *Applied Optics*, 57:4618, 6 2018.
87. T D Arber, K Bennett, C S Brady, A Lawrence-Douglas, M G Ramsay, N J Sircombe, P Gillies, R G Evans, H Schmitz, A R Bell, and C P Ridgers. Contemporary particle-in-cell approach to laser-plasma modelling. *Plasma Physics and Controlled Fusion*, 57(11):113001, 2015.
88. WILLIAM KRUER. *PHYSICS OF LASER PLASMA INTERACTIONS*. CRC Press, 2019.
89. N.G. Denisov. On a singularity of the field on an electromagnetic wave propagated in an inhomogeneous plasma. *J. Exp. Theor. Phys.*, 4(4):544, 1957.
90. P. Stampfli and K. H. Bennemann. Dynamical theory of the laser-induced lattice instability of silicon. *Physical Review B*, 46(17):10686–10692, 1992.
91. Baerbel Rethfeld, Dmitriy S Ivanov, Martin E Garcia, and Sergei I Anisimov. Modelling ultrafast laser ablation. *Journal of Physics D: Applied Physics*, 50(19):193001, 2017.
92. Thomas Winkler, Lasse Haahr-Lillevang, Cristian Sarpe, Bastian Zielinski, Nadine Götte, Arne Senftleben, Peter Balling, and Thomas Baumert. Laser amplification in excited dielectrics. *Nature Physics*, 14(1):74–79, 2017-09.
93. S.S. Mao, F. Quéré, S. Guizard, X. Mao, R.E. Russo, G. Petite, and P. Martin. Dynamics of femtosecond laser interactions with dielectrics. *Appl. Phys. A*, 79(7):1695–1709, jun 2004.
94. R. G. Kraus, S. T. Stewart, D. C. Swift, C. A. Bolme, R. F. Smith, S. Hamel, B. D. Hammel, D. K. Spaulding, D. G. Hicks, J. H. Eggert, and G. W. Collins. Shock vaporization of silica and the thermodynamics of planetary impact events. *Journal of Geophysical Research: Planets*, 117(E9):n/a–n/a, 2012.
95. E. N. Glezer and E. Mazur. Ultrafast-laser driven micro-explosions in transparent materials. *Appl. Phys. Lett.*, 71(7):882, 1997.
96. Romain Beuton, Benoît Chimier, Jérôme Breil, David Hébert, Pierre Henri Maire, and Guillaume Duchateau. Thermo-elasto-plastic simulations of femtosecond laser-induced structural modifications: Application to cavity formation in fused silica. *Journal of Applied Physics*, 122, 11 2017.
97. Manoj Kumar Bhuyan, Praveen Kumar Velpula, Madhura Somayaji, Jean Philippe Colombier, and Razvan Stoian. 3d nano-fabrication using controlled Bessel-glass interaction in ultra-fast modes. *Journal of Laser Micro Nanoengineering*, 12:274–280, 12 2017.
98. M. K. Bhuyan, M. Somayaji, A. Mermillod-Blondin, F. Bourquard, J. P. Colombier, and R. Stoian. Ultrafast laser nanostructuring in bulk silica, a "slow" microexplosion. *Optica*, 4(8):951, aug 2017.
99. M. Bonitz, T. Dornheim, Zh. A. Moldabekov, S. Zhang, P. Hamann, H. Kählert, A. Filinov, K. Ramakrishna, and J. Vorberger. Ab initio simulation of warm dense matter. *Phys. Plasmas*, 27(4):042710, 2020.
100. Koji Sugioka and Ya Cheng. Ultrafast lasers—reliable tools for advanced materials processing. *Light: Science & Applications*, 3(4):e149–e149, 2014.
101. Mangirdas Malinauskas, Albertas Žukauskas, Satoshi Hasegawa, Yoshio Hayasaki, Vygantas Mizeikis, Ričardas Buividas, and Saulius Juodkazis. Ultrafast laser processing of materials: From science to industry. *Light: Science and Applications*, 5, 8 2016.
102. Felix Sima and Koji Sugioka. Ultrafast laser manufacturing of nanofluidic systems. *Nanophotonics*, 10:2389–2406, 7 2021.
103. Maria Manousidaki, Dimitrios G. Papazoglou, Maria Farsari, and Stelios Tzortzakis. Long-scale multiphoton polymerization voxel growth investigation using engineered Bessel beams. *Optical Materials Express*, 9:2838, 7 2019.
104. He Cheng, Chun Xia, Stephen M. Kuebler, and Xiaoming Yu. Aberration correction for slm-generated Bessel beams propagating through tilted interfaces. *Optics Communications*, 475, 11 2020.
105. C. Mauclair, A. Mermillod-Blondin, K. Mishchik, J. Bonse, A. Rosenfeld, J. P. Colombier, and R. Stoian. Excitation and relaxation dynamics in ultrafast laser irradiated optical glasses. *High Power Laser Science and Engineering*, 4, 2016.

106. Xu Wang, Guodong Zhang, Yunjie Zhang, Xiaoping Xie, Guanghua Cheng, and Weinan Li. Photochemical response triggered by ultrashort laser Gaussian -Bessel beams in photo-thermo-refractive glass. *Optics Express*, 28:31093, 10 2020.
107. Mindaugas Mikutis, Tadas Kudrius, Gintas Šlekys, Domas Paipulas, and Saulius Juodkazis. High 90% efficiency bragg gratings formed in fused silica by femtosecond Gauss-Bessel laser beams. *Optical Materials Express*, 3(11):1862, oct 2013.
108. Yu Matushiro and Wataru Watanabe. Femtosecond laser processing of polymethyl methacrylate with an axicon. *Journal of Laser Micro Nanoengineering*, 11:59–65, 2016.
109. Wataru Watanabe, Yu Matushiro, Koji Hatanaka, and Saulius Juodkazis. Regeneration of a grating in pmma inscribed by femtosecond laser Bessel beam. *Journal of Laser Micro Nanoengineering*, 12:102–106, 2017.
110. Kentaro Homma and Wataru Watanabe. Fabrication of pdms-based volume bragg gratings by stitching of femtosecond laser filament. *Japanese Journal of Applied Physics*, 60, 3 2021.
111. Darius Gailevičius, Vytautas Purlys, and Kestutis Staliunas. Photonic crystal spatial filters fabricated by femtosecond pulsed Bessel beam. *Optics Letters*, 44:4969, 10 2019.
112. Qi Sun, Timothy Lee, Martynas Beresna, and Gilberto Brambilla. Control of laser induced cumulative stress for efficient processing of fused silica. *Scientific Reports*, 10, 12 2020.
113. Zhi Wang, Lan Jiang, Xiaowei Li, Andong Wang, Zhulin Yao, Kaihu Zhang, and Yongfeng Lu. High-throughput microchannel fabrication in fused silica by temporally shaped femtosecond laser Bessel-beam-assisted chemical etching. *Opt. Lett.*, 43(1):98, 2017.
114. Dongkai Chu, Peng Yao, Xiaoyan Sun, Kai Yin, and Chuanzhen Huang. Ablation enhancement of fused silica glass by femtosecond laser double-pulse Bessel beam. *Journal of the Optical Society of America B*, 37:3535, 11 2020.
115. Anton Rudenko, Jean Philippe Colombier, and Tatiana E. Itina. Influence of polarization state on ultrafast laser-induced bulk nanostructuring. *Journal of Laser Micro Nanoengineering*, 11:304–311, 2016.
116. G. Cheng, A. Rudenko, C. D'Amico, T. E. Itina, J. P. Colombier, and R. Stoian. Embedded nanogratings in bulk fused silica under non-diffractive Bessel ultrafast laser irradiation. *Applied Physics Letters*, 110, 6 2017.
117. Takayuki Tamaki, Wataru Watanabe, Junji Nishii, and Kazuyoshi Itoh. Welding of transparent materials using femtosecond laser pulses. *Japanese Journal of Applied Physics*, 44(No. 22):L687–L689, may 2005.
118. Wataru Watanabe, Satoshi Onda, Takayuki Tamaki, Kazuyoshi Itoh, and Junji Nishii. Space-selective laser joining of dissimilar transparent materials using femtosecond laser pulses. *Applied Physics Letters*, 89(2):021106, jul 2006.
119. S. Richter, F. Zimmermann, R. Eberhardt, A. Tünnermann, and S. Nolte. Toward laser welding of glasses without optical contacting. *Applied Physics A*, 121(1):1–9, aug 2015.
120. Guodong Zhang, Razvan Stoian, Wei Zhao, and Guanghua Cheng. Femtosecond laser bessel beam welding of transparent to non-transparent materials with large focal-position tolerant zone. *Optics Express*, 26(2):917, 2018.
121. Sebastian Hecker, Markus Blothe, and Thomas Graf. Reproducible process regimes during glass welding by bursts of subpicosecond laser pulses. *Applied Optics*, 59:11382, 12 2020.
122. G. Martin, M. Bhuyan, J. Troles, C. D'Amico, R. Stoian, and E. Le Coarer. Near infrared spectro-interferometer using femtosecond laser written gls embedded waveguides and nano-scatterers. *Optics Express*, 25:8386, 4 2017.
123. Ciro D'amico, Guillermo Martin, Johann Troles, Guanghua Cheng, and Razvan Stoian. Multiscale laser written photonic structures in bulk chalcogenide glasses for infrared light transport and extraction. *Photonics*, 8, 6 2021.
124. G. Zhang, G. Cheng, M. Bhuyan, C. D'Amico, and R. Stoian. Efficient point-by-point bragg gratings fabricated in embedded laser-written silica waveguides using ultrafast Bessel beams. *Optics Letters*, 43:2161, 5 2018.
125. Keivan Mahmoud Aghdami, Abdullah Rahnama, Erden Ertorer, and Peter R. Herman. Laser nano-filament explosion for enabling open-grating sensing in optical fibre. *Nature Communications*, 12(1), 2021.

126. Xin Liu, Nicolas Sanner, Marc Sentis, Razvan Stoian, Wei Zhao, Guanghua Cheng, and Olivier Utéza. Front-surface fabrication of moderate aspect ratio micro-channels in fused silica by single picosecond Gaussian –Bessel laser pulse. *Applied Physics A: Materials Science and Processing*, 124, 2 2018.
127. X. Liu, Q. Li, A. Sikora, M. Sentis, O. Utéza, R. Stoian, W. Zhao, G. Cheng, and N. Sanner. Truncated Gaussian -Bessel beams for short-pulse processing of small-aspect-ratio micro-channels in dielectrics. *Optics Express*, 27:6996, 3 2019.
128. Ottavia Jedrkiewicz, Davide Valetti, and Paolo Di Trapani. Etching and drilling of through-holes in thin glass by means of picosecond Bessel beams. *SN Applied Sciences*, 1, 10 2019.
129. V. V. Belloni, V. Sabonis, P. Di Trapani, and O. Jedrkiewicz. Burst mode versus single-pulse machining for Bessel beam micro-drilling of thin glass: study and comparison. *SN Applied Sciences*, 2:1589, 9 2020.
130. Valeria V. Belloni, Monica Bollani, Shane M. Eaton, Paolo Di Trapani, and Ottavia Jedrkiewicz. Micro-hole generation by high-energy pulsed Bessel beams in different transparent materials. *Micromachines*, 12:455, 4 2021.
131. Simas Butkus, Domas Paipulas, Romualdas Sirutkaitis, Eugenijus Gaižauskas, and Valdas Sirutkaitis. Rapid cutting and drilling of transparent materials via femtosecond laser filamentation. *Journal of Laser Micro Nanoengineering*, 9:213–220, 2014.
132. Yusuke Ito, Reina Yoshizaki, Naoyuki Miyamoto, and Naohiko Sugita. Ultrafast and precision drilling of glass by selective absorption of fiber-laser pulse into femtosecond-laser-induced filament. *Applied Physics Letters*, 113, 8 2018.
133. Yusuke Ito, Rin Shinomoto, Akinori Otsu, Keisuke Nagato, and Naohiko Sugita. Dynamics of pressure waves during femtosecond laser processing of glass. *Optics Express*, 27:29158, 9 2019.
134. Masayoshi Kumagai, Naoki Uchiyama, Etusji Ohmura, Ryuji Sugiura, Kazuhiro Atsumi, and Kenshi Fukumitsu. Advanced dicing technology for semiconductor wafer—stealth dicing. *IEEE Transactions on Semiconductor Manufacturing*, 20(3):259–265, 2007.
135. Konstantin Mishchik, Bruno Chassagne, Clémentine Javaux-Léger, Clemens Hönninger, Eric Mottay, Rainer Kling, and John Lopez. Dash line glass- and sapphire-cutting with high power USP laser. In Alexander Heisterkamp, Peter R. Herman, Michel Meunier, and Stefan Nolte, editors, *Frontiers in Ultrafast Optics: Biomedical, Scientific, and Industrial Applications XVI*. SPIE, 2016.
136. Farid Ahmed, Man Seop Lee, Hitoshi Sekita, Tetsumi Sumiyoshi, and Masanao Kamata. Display glass cutting by femtosecond laser induced single shot periodic void array. *Applied Physics A*, 93(1):189–192, jun 2008.
137. Wu-Jung Tsai, Chun-Jen Gu, Chung-Wei Cheng, and Ji-Bin Horng. Internal modification for cutting transparent glass using femtosecond Bessel beams. *Optical Engineering*, 53:051503, 12 2013.
138. M. K. Bhuyan, O. Jedrkiewicz, V. Sabonis, M. Mikutis, S. Recchia, A. Aprea, M. Bollani, and P. Di Trapani. High-speed laser-assisted cutting of strong transparent materials using picosecond Bessel beams. *Applied Physics A: Materials Science and Processing*, 120:443–446, 8 2015.
139. Craig Ungaro, Nikolay Kaliteevskiy, Petr Sterlingov, Viacheslav V. Ivanov, A. Boh Ruffin, Ralf J. Terbrueggen, and Nickolaos Savidis. Using phase-corrected Bessel beams to cut glass substrates with a chamfered edge. *Applied Optics*, 60:714, 1 2021.
140. Jianzhao Li, Erden Ertorer, and Peter R. Herman. Ultrafast laser burst-train filamentation for non-contact scribing of optical glasses. *Optics Express*, 27:25078, 9 2019.
141. Juozas Dudutis, Jokūbas Pipiras, Rokas Stonys, Eimantas Daknys, Artūras Kilikevičius, Albinas Kasparaitis, Gediminas Račiukaitis, and Paulius Gečys. In-depth comparison of conventional glass cutting technologies with laser-based methods by volumetric scribing using Bessel beam and rear-side machining. *Optics Express*, 28:32133, 10 2020.
142. Klaus Bergner, Michael Müller, Robert Klas, Jens Limpert, Stefan Nolte, and Andreas Tünnerman. Scaling ultrashort laser pulse induced glass modifications for cleaving applications. *Applied Optics*, 57:5941, 7 2018.

143. A. Feuer, J. U. Thomas, C. Freitag, R. Weber, and T. Graf. Single-pass laser separation of 8 mm thick glass with a millijoule picosecond pulsed Gaussian –Bessel beam. *Applied Physics A: Materials Science and Processing*, 125, 5 2019.
144. M. Jenne, F. Zimmermann, D. Flamm, D. Großmann, J. Kleiner, M. Kumkar, and S. Nolte. Multi pulse pump-probe diagnostics for development of advanced transparent materials processing. *Journal of Laser Micro Nanoengineering*, 13:273–279, 12 2018.
145. Michael Jenne, Daniel Flamm, Max Faber, Daniel Grossmann, Jonas Kleiner, Felix Zimmermann, Malte Kumkar, and Stefan Nolte. Pump-probe microscopy of tailored ultrashort laser pulses for glass separation processes. page 52. SPIE-Intl Soc Optical Eng, 3 2019.
146. Tongwei Liu, Haiying Wei, Jiazhu Wu, Jiangang Lu, and Yi Zhang. Modulation of crack formation inside single-crystal sapphire using ultrafast laser Bessel beams. *Optics and Laser Technology*, 136, 4 2021.
147. R. Meyer, M. Jacquot, R. Giust, J. Safioui, L. Rapp, L. Furfaro, P.-A. Lacourt, J. M. Dudley, and F. Courvoisier. Single-shot ultrafast laser processing of high-aspect-ratio nanochannels using elliptical Bessel beams. *Optics Letters*, 42(21):4307, oct 2017.
148. Daniel Flamm, Keyou Chen, Michael Jenne, Marcel Schäfer, Daniel G. Grossmann, Julian Hellstern, Christoph Tillkorn, and Malte Kumkar. Generalized non-diffracting beams for ultrafast materials processing. page 34. SPIE-Intl Soc Optical Eng, 3 2020.
149. Michael Jenne, Daniel Flamm, Keyou Chen, Marcel Schäfer, Malte Kumkar, and Stefan Nolte. Facilitated glass separation by asymmetric Bessel-like beams. *Optics Express*, 28:6552, 3 2020.
150. Juozas Dudutis, Rokas Stonys, Gediminas Račiukaitis, and Paulius Gečys. Aberration-controlled Bessel beam processing of glass. *Optics Express*, 26:3627, 2 2018.
151. Juozas Dudutis, Rokas Stonys, Gediminas Račiukaitis, and Paulius Gečys. Glass dicing with elliptical Bessel beam. *Optics and Laser Technology*, 111:331–337, 4 2019.
152. R. Meyer, R. Giust, M. Jacquot, J. M. Dudley, and F. Courvoisier. Submicron-quality cleaving of glass with elliptical ultrafast Bessel beams. *Applied Physics Letters*, 111(23):231108, dec 2017.
153. R. Beuton, B. Chimier, J. Breil, D. Hébert, K. Mishchik, J. Lopez, P. H. Maire, and G. Duchateau. Thermo-elasto-plastic simulations of femtosecond laser-induced multiple-cavity in fused silica. *Applied Physics A: Materials Science and Processing*, 124, 4 2018.
154. Michael Jenne, Daniel Flamm, Taoufiq Ouaj, Julian Hellstern, Jonas Kleiner, Daniel Grossmann, Maximilian Koschig, Myriam Kaiser, Malte Kumkar, and Stefan Nolte. High-quality tailored-edge cleaving using aberration-corrected Bessel-like beams. *Optics Letters*, 43(13):3164, jun 2018.
155. Daniel Flamm, Daniel G. Grossmann, Marc Sailer, Myriam Kaiser, Felix Zimmermann, Keyou Chen, Michael Jenne, Jonas Kleiner, Julian Hellstern, Christoph Tillkorn, Dirk H. Sutter, and Malte Kumkar. Structured light for ultrafast laser micro- and nanoprocessing. *Optical Engineering*, 60, 2 2021.
156. Georgios A. Siviloglou and Demetrios N. Christodoulides. Accelerating finite energy airy beams. *Optics Letters*, 32(8):979, 2007.
157. P. Polynkin, M. Kolesik, J. V. Moloney, G. A. Siviloglou, and D. N. Christodoulides. Curved plasma channel generation using ultraintense airy beams. *Science*, 324(5924):229–232, 2009-04.
158. M. Clerici, Y. Hu, P. Lassonde, C. Milian, A. Couairon, D. N. Christodoulides, Z. Chen, L. Razzari, F. Vidal, F. Legare, D. Faccio, and R. Morandotti. Laser-assisted guiding of electric discharges around objects. *Science Advances*, 1(5):e1400111–e1400111, 2015.
159. Sophie Vo, Kyle Fuerschbach, Kevin P. Thompson, Miguel A. Alonso, and Jannick P. Rolland. Airy beams: a geometric optics perspective. *Journal of the Optical Society of America A*, 27(12):2574, 2010.
160. Elad Greenfield, Mordechai Segev, Wiktor Walasik, and Oren Raz. Accelerating light beams along arbitrary convex trajectories. *Phys. Rev. Lett.*, 106(21):213902, 2011.
161. L. Froehly, F. Courvoisier, A. Mathis, M. Jacquot, L. Furfaro, R. Giust, P. A. Lacourt, and J. M. Dudley. Arbitrary accelerating micron-scale caustic beams in two and three dimensions. *Opt. Express*, 19(17):16455, 2011.

162. F. Courvoisier, A. Mathis, L. Froehly, R. Giust, L. Furfaro, P. A. Lacourt, M. Jacquot, and J. M. Dudley. Sending femtosecond pulses in circles: highly nonparaxial accelerating beams. *Optics Letters*, 37(10):1736, 2012.
163. A. Mathis, F. Courvoisier, R. Giust, L. Furfaro, M. Jacquot, L. Froehly, and J. M. Dudley. Arbitrary nonparaxial accelerating periodic beams and spherical shaping of light. *Optics Letters*, 38(13):2218, 2013.
164. Miguel A. Alonso and Miguel A. Bandres. Generation of nonparaxial accelerating fields through mirrors. i: Two dimensions. *Opt. Express*, 22(6):7124–7132, Mar 2014.
165. A. Mathis, L. Froehly, L. Furfaro, M. Jacquot, J. M. Dudley, and F. Courvoisier. Direct machining of curved trenches in silicon with femtosecond accelerating beams. *JEOS:RP*, 8, 2013.
166. David Sohr, Jens Ulrich Thomas, and Stefan Skupin. Shaping convex edges in borosilicate glass by single pass perforation with an airy beam. *Optics Letters*, 46:2529, 5 2021.
167. Daniel Flamm, Myriam Kaiser, Marvin Feil, Max Kahmann, Michael Lang, Jonas Kleiner, and Tim Hesse. Protecting the edge: Ultrafast laser modified c-shaped glass edges. 2021.
168. V. Jukna, C. Milián, C. Xie, T. Itina, J. Dudley, F. Courvoisier, and A. Couairon. Filamentation with nonlinear bessel vortices. *Opt. Express*, 22(21):25410, 2014.
169. Chen Xie, Vytautas Jukna, Carles Milián, Remo Giust, Ismail Ouadghiri-Idrissi, Tatiana Itina, John M. Dudley, Arnaud Couairon, and Francois Courvoisier. Tubular filamentation for laser material processing. *Sci. Rep.*, 5:8914, mar 2015.
170. Weibo Cheng and Pavel Polynkin. Micromachining of borosilicate glass surfaces using femtosecond higher-order bessel beams. *Journal of the Optical Society of America B*, 31(11):C48, 2014.
171. Ottavia Jedrkiewicz, Simone Bonanomi, Marco Selva, and Paolo Di Trapani. Experimental investigation of high aspect ratio tubular microstructuring of glass by means of picosecond Bessel vortices. *Applied Physics A: Materials Science and Processing*, 120:385–391, 7 2015.
172. Justas Baltrukonis, Orestas Ulčinas, Sergej Orlov, and Vytautas Jukna. Void and micro-crack generation in transparent materials with high-energy first-order vector Bessel beam. *Journal of the Optical Society of America B*, 37:2121, 7 2020.
173. Ernestas Nacius, Pavel Gotovski, Orestas Ulcinas, Sergejus Orlovas, Antanas Urbas, and Vytautas Jukna. Spatially displaced and superposed Bessel beams for transparent material laser micro-processing. *Journal of the Optical Society of America B*, 11 2021.
174. Paulius Šlevas, Sergej Orlov, Ernestas Nacius, and Orestas Ulčinas. Azimuthally modulated axicon vortical beams for laser microprocessing. *Optics Communications*, 505, 2 2022.
175. Sergej Orlov, Alfonsas Juršenas, and Ernestas Nacius. Optical Bessel-like beams with engineered axial phase and intensity distribution. *Journal of Laser Micro Nanoengineering*, 13:244–248, 12 2018.
176. Xiaoming Yu, Carlos A. Trallero-Herrero, and Shuting Lei. Materials processing with superposed Bessel beams. *Applied Surface Science*, 360:833–839, 1 2016.
177. Liang Yang, Dongdong Qian, Chen Xin, Zhijiang Hu, Shengyun Ji, Dong Wu, Yanlei Hu, Jiawen Li, Wenhao Huang, and Jiaru Chu. Two-photon polymerization of microstructures by a non-diffraction multifoci pattern generated from a superposed Bessel beam. *Optics Letters*, 42:743, 2 2017.
178. Yoshihiko Arita, Junhyung Lee, Haruki Kawaguchi, Reimon Matsuo, Katsuhiko Miyamoto, Kishan Dholakia, and Takashige Omatsu. Photopolymerization with high-order Bessel light beams. *Optics Letters*, 45, 2020.
179. Alessandro Zannotti, Cornelia Denz, Miguel A. Alonso, and Mark R. Dennis. Shaping caustics into propagation-invariant light. *Nature Communications*, 11(1), 2020-07.
180. Thomas Dietz, Michael Jenne, Dominik Bauer, Michael Scharun, Dirk Sutter, and Alexander Killi. Ultrafast thin-disk multi-pass amplifier system providing 19 kw of average output power and pulse energies in the 10 mj range at 1 ps of pulse duration for glass-cleaving applications. *Optics Express*, 28:11415, 4 2020.
181. Arturas Vailionis, Eugene G. Gamaly, Vygantas Mizeikis, Wenge Yang, Andrei V. Rode, and Saulius Juodkazis. Evidence of superdense aluminium synthesized by ultrafast microexplosion. *Nature Communications*, 2(1), aug 2011.